City Research Online

City, University of London Institutional Repository

Citation: Ballotta, L. and Kyriakou, I. (2014). Monte carlo simulation of the CGMY process and option pricing. Journal of Futures Markets, doi: 10.1002/fut.21647

This is the accepted version of the paper.

This version of the publication may differ from the final published version.

Permanent repository link: https://openaccess.city.ac.uk/id/eprint/3976/

Link to published version: http://dx.doi.org/10.1002/fut.21647

Copyright: City Research Online aims to make research outputs of City, University of London available to a wider audience. Copyright and Moral Rights remain with the author(s) and/or copyright holders. URLs from City Research Online may be freely distributed and linked to.

Reuse: Copies of full items can be used for personal research or study, educational, or not-for-profit purposes without prior permission or charge. Provided that the authors, title and full bibliographic details are credited, a hyperlink and/or URL is given for the original metadata page and the content is not changed in any way.

City Research Online: http://openaccess.city.ac.uk/ publications@city.ac.uk

Monte Carlo simulation of the CGMY process and option pricing

Laura Ballotta† and Ioannis Kyriakou‡

16 May 2013

Abstract

We present a joint Monte Carlo-Fourier transform sampling scheme for pricing derivative products under a CGMY model exhibiting jumps of infinite activity and finite or infinite variation. The approach relies on numerical transform inversion with computable error estimates, which allow generating the unknown cumulative distribution function (CDF) of the CGMY process increments at the desired accuracy level. We use this to generate samples and simulate the entire trajectory of the process without need of truncating the process small jumps. We illustrate the computational efficiency of the proposed method by comparing it to the existing methods in the literature on pricing a wide range of option contracts, including path-dependent univariate and multivariate products.

The authors would like to thank Gianluca Fusai for interesting comments to a previous version of this paper, Russell Gerrard for his valuable contribution that helped improve the paper, Gerald Rickayzen for useful discussions, and Michele Bianchi, Reiichiro Kawai and Hiroki Masuda for useful suggestions on the implementation of the SR and AR sampling schemes. Usual caveat applies.

JEL Classification: G12, G13, C63

†Corresponding author. Cass Business School, City University London, 106 Bunhill Row, London EC1Y 8TZ, UK. Tel.: +44 (0) 20 7040 8954, Fax: +44 (0) 20 7040 8881, E-mail: L.Ballotta@city.ac.uk

‡Cass Business School, City University London, 106 Bunhill Row, London EC1Y 8TZ, UK. Tel.: +44 (0) 20 7040 8738, Fax: +44 (0) 20 7040 8572, E-mail: Ioannis.Kyriakou@city.ac.uk

1 Introduction

In this paper we present an efficient Monte Carlo simulation scheme coupled with Fourier transform, which we name MC-FT, for the pricing of single and multi-asset option contracts when the underlying is governed by a CGMY process.

The CGMY process has been introduced by Carr et al. (2002) with the aim to provide a model for the dynamic of equity log-returns which is rich enough to accommodate jumps of finite or infinite activity, and finite or infinite variation. Their empirical analysis shows, in fact, that risk neutral processes are mainly of infinite activity with finite variation, while infinite variation may be prevalent in the corresponding statistical processes. The CGMY process has also been reported to perform consistently better than other Lévy processes when extended via a random time change to include stochastic volatility (e.g., see Carr et al., 2003).

In recent years, numerical integration/transform techniques have proved very fast and accurate on pricing a wide range of single-asset derivative products with path-dependence and early-exercise features written on Lévy driven underlying price processes with known characteristic functions (e.g., see Chung et al., 2010; Lord et al., 2008; Feng and Linetsky, 2008; Černý and Kyriakou, 2011). However, these techniques often become impractical when tackling high dimensional problems, such as multi-asset contracts with path-dependent payoffs (like, e.g., Asian basket options); in such cases, Monte Carlo simulation is generally the method of choice. Monte Carlo simulation of the CGMY process, though, is not straightforward due to the fact that its cumulative distribution function (as well as its density function) is not available in closed form.

Monte Carlo simulation of the CGMY process has been tackled in the literature specifically by Madan and Yor (2008), Poirot and Tankov (2006) and Rosiński (2007). In details, Madan and Yor (2008) present a Monte Carlo strategy for the CGMY process based on a Brownian subordination construction of the process proposed by the same authors. Rosiński (2007) proposes an alternative approach which uses a representation of the CGMY process

as an infinite sum of a mixture of independent random variables whose exact simulation is straightforward. However, the first method entails truncating jumps of size smaller than a threshold level and replacing these by their expectation, while the second one requires truncation of the infinite sum. As a consequence, the resulting Monte Carlo price estimates are affected by an approximation bias which may be substantial and, at the same time, difficult to quantify. In order to avoid such errors, Poirot and Tankov (2006) construct a new probability measure under which the original CGMY reduces to a stable process whose exact simulation is well established. Although faster in execution, the method of Poirot and Tankov (2006) does not provide access to the entire trajectory of the process precluding the pricing of path-dependent products; further, the extension of this approach to a multidimensional setting is not straightforward.

Other relevant simulation methods available in the literature are based on acceptance-rejection sampling (e.g., see Devroye, 1981; Baeumer and Meerschaert, 2010), and Gaussian approximation of the small jump part (see Asmussen and Rosiński, 2001). Kawai and Masuda (2011) provide a comparison of these methods in terms of acceptance rate, approximation error and computing time; it is shown that the acceptance-rejection sampling scheme of Baeumer and Meerschaert (2010) is the simplest and most efficient to use for any given computing budget, especially when simulating CGMY increments over small time steps. The method, though, is only exact for a CGMY process with infinite activity and finite variation, while an approximation error is introduced in the infinite variation case.

Another class of simulation methods available for distribution laws known only through the associated characteristic functions couples Monte Carlo principles with transform inversion. Applications have been shown for common Lévy processes by Glasserman and Liu (2010) and Chen et al. (2012) amongst others, but also for the Heston stochastic volatility model by Broadie and Kaya (2006) and Glasserman and Kim (2009).

In this paper we build on the latter stream of contributions and focus on the nontrivial case of the CGMY process. We propose and analyze a method that only requires knowledge of the properties of the CGMY characteristic function, and does not rely on possibly arbi-

trary truncation rules. In addition, we study the representation of the CGMY process as subordinated Brownian motion of Madan and Yor (2008), which also admits a closed form expression for the characteristic function of the subordinator. This representation is usually considered in view of constructing multivariate versions of the CGMY process (e.g., see Madan and Yor, 2008; Luciano and Semeraro, 2010). We examine the behaviour of the two characteristic functions when the CGMY exhibits jumps of finite activity, infinite activity with finite variation and infinite variation; of particular interest is the case of infinite variation which is less frequently met in the literature of transform pricing techniques (e.g., see Feng and Linetsky, 2008; Chen et al., 2012; Cai et al., 2013). For a CGMY process of infinite activity with finite or infinite variation, we prove sufficient conditions for the existence of computable exponentially decaying bounds for the errors induced by retrieving the CDF using numerical transform inversion. This allows us to compute the values of the CDF at the desired accuracy for later use in the simulation part, making the proposed simulation scheme virtually bias free. Finally, we show that in the finite activity case the characteristic function is not absolutely integrable precluding transform inversion. However, this case is of less interest as CGMY admits an explicit representation as a compound Poisson process which can be simulated exactly.

The remainder of this paper is organized as follows. Section 2 contains preliminaries. Section 3 reviews the CGMY process. Section 4 presents the main theoretical results of the paper. Further, the practical application to numerical evaluation of the distribution function and the use in the simulation of the CGMY process is outlined. In Section 5, we apply the proposed sampling method on pricing European plain vanilla, Asian and barrier options with discrete monitoring. We highlight the benefits of the proposed approach by comparing it to the existing Monte Carlo methods of Poirot and Tankov (2006), Madan and Yor (2008), Baeumer and Meerschaert (2010) and Rosiński (2007). In Section 6, we extend to multivariate products. Section 7 concludes. All the proofs are deferred to the appendices.

2 Preliminaries

2.1 Regularizing distribution functions

Assume some random variable X with (unknown) continuous cumulative distribution function F. For $D > 0$ consider the auxiliary function

$$F_r(x) = F(x) - \frac{1}{2}F(x - D) - \frac{1}{2}F(x + D) \tag{1}$$

(see Hughett, 1998), which is regularized in the sense that it decays to zero as $|x| \to \infty$. Then, for sufficiently large D, $F(x)$ approaches $F_r(x) + 1/2$ for fixed x. Hence, providing that $F_r(x)$ is known (see Section 2.2), it can be used to compute $F(x)$ subject to a so-called regularization error given by $|F(x) - F_r(x) - 1/2|$. In the following, we extend previous work by Hughett (1998) based on polynomial decay of $1 - F(x)$ and $F(-x)$ to exponential decay as $x \to \infty$, providing that exponential moments of the distribution exist in an interval containing the origin, and use these to derive a tight explicit bound for the regularization error. Assume that

$$E(e^{-yX}) < \infty \tag{2}$$

for all $y \in (a^-, a^+)$ with $-\infty < a^- \leq 0 \leq a^+ < \infty$. For any nonnegative function g the inequality

$$P(g(X) \geq \gamma) \leq E\left(g(X)\right)\gamma^{-1}$$

holds for any $\gamma > 0$ (e.g., see Abramowitz and Stegun, 1968, p. 931), from which it follows that

$$1 - F(x) = P(X \geq x) = P(e^{\alpha X} \geq e^{\alpha x}) \leq E(e^{\alpha X})e^{-\alpha x}, \tag{3}$$

$$F(-x) = P(-X \geq x) = P(e^{-\alpha X} \geq e^{\alpha x}) \leq E(e^{-\alpha X})e^{-\alpha x} \tag{4}$$

for $\alpha > 0$ such that $[-\alpha, \alpha] \subset (a^-, a^+)$. Then, for $|x| \leq D/2$ so that $D \pm x \geq D/2 > 0$, the regularization error of replacing F by $F_r + 1/2$ in (1) can be bounded as follows

$$\begin{aligned} \left| F(x) - F_r(x) - \frac{1}{2} \right| &\leq \frac{1}{2} \left| F(-(D-x)) \right| + \frac{1}{2} \left| 1 - F(x+D) \right| \\ &\leq \frac{1}{2} \left(E(e^{-\alpha X}) + E(e^{\alpha X}) \right) e^{-\alpha D/2}. \end{aligned} \tag{5}$$

2.2 Fourier inversion formula of the distribution function

The regularized distribution function F_r is known through its Fourier transform (e.g., see Hughett, 1998) given by the continuous function

$$\phi_r(u) := \int_{\mathbb{R}} e^{iux} F_r(x) dx = \begin{cases} -\frac{1-\cos(uD)}{iu} \phi(u) & u \neq 0 \\ 0 & u = 0 \end{cases}, \tag{6}$$

where

$$\phi(u) := E(e^{iuX}).$$

To invert the Fourier transform (6), from, e.g., Goldberg (1961), we require that

$$\int_{\mathbb{R}} |\phi_r(u)| du = \int_{\mathbb{R}} \frac{1 - \cos(uD)}{|u|} |\phi(u)| du \leq D \int_{\mathbb{R}} |\phi(u)| du < \infty, \tag{7}$$

where we have used $(1 - \cos u)/|u| \leq 1$ for $u \in \mathbb{R}$. Assuming (7) holds, we can invert (6) and write

$$F_r(x) = \frac{1}{2\pi} \int_{\mathbb{R}} e^{-iux} \phi_r(u) du. \tag{8}$$

In practice, to evaluate F_r, we need to truncate the infinite integration domain in (8) by choosing a sufficiently large $L > 0$ and work on the truncated finite interval $[-L/2, L/2]$. To this end, let us introduce

$$F_c(x) = \frac{1}{2\pi} \int_{-L/2}^{L/2} e^{-iux} \phi_r(u) du, \tag{9}$$

then the resulting truncation error is bounded by

$$|F_r(x) - F_c(x)| \leq \frac{1}{\pi} \int_{u>L/2}^{\infty} |\phi_r(u)| du \leq \frac{D}{\pi} \int_{L/2}^{\infty} |\phi(u)| du. \tag{10}$$

From (10) the truncation error depends on the tail behaviour of the characteristic function. In order to bound the truncation error, it is sufficient that

$$|\phi(u)| \leq B e^{-b|u|^{\beta}} \tag{11}$$

for $B, b, \beta > 0$. Then,

$$|F_r(x) - F_c(x)| \leq \frac{D}{\pi} \int_{L/2}^{\infty} B e^{-bu^{\beta}} du = \frac{DB}{\pi \beta b^{1/\beta}} \Gamma(1/\beta, bL^{\beta} 2^{-\beta}) = o(L^{1-\beta} e^{-bL^{\beta} 2^{-\beta}}), \tag{12}$$

where $\Gamma(\varepsilon, x) = \int_x^{\infty} e^{-t} t^{\varepsilon - 1} dt$ denotes the upper incomplete gamma function and the last equality follows from $\lim_{x \to \infty} \Gamma(\varepsilon, x)/(x^{\varepsilon - 1} e^{-x}) = 1$ (e.g., see Abramowitz and Stegun, 1968, p. 263). Hence, the truncation error decays exponentially in L; however, bound (11) does not hold or is not possible to derive always. A less sharp, still useful, alternative applies in the case of selfdecomposable laws with Lévy densities of the special form $\nu(x) = k(x)/|x|$, where $k(x)$ is a nonnegative function increasing for negative x and decreasing for positive x (see Sato, 1999, Corollary 15.11). Lemma 28.5 in Sato (1999) shows that these laws admit characteristic functions decaying as $|u|^{-\beta}$ as $|u| \to \infty$ for $1 < \beta < \gamma$, where $\gamma := k(0+) + k(0-)$. Therefore, for $B > 0$

$$|\phi(u)| \leq B|u|^{-\beta} \tag{13}$$

and

$$|F_r(x) - F_c(x)| \leq \frac{D}{\pi} \int_{L/2}^{\infty} B u^{-\beta} du = \frac{DB 2^{\beta - 1}}{\pi(\beta - 1)} L^{1-\beta} = o(L^{1-\beta}). \tag{14}$$

We note that characteristic functions with exponential decay (11), or polynomial decay (13) with $\beta > 1$ suffice to guarantee that ϕ_r is absolutely integrable, i.e., (7) is satisfied.

To compute the truncated inverse Fourier transform integral (9), we employ numerical integration in the Fourier space which generates, additionally, discretization error. Based on the study of Feng and Linetsky (2008), it is possible to approximate integral (9) using simple rules with error converging exponentially to zero in $1/h$ where h denotes the discretization spacing. More specifically, given some evenly spaced grid $\mathbf{u} := \{(j - N/2)h\}_{j=0}^{N-1}$, we approximate $F_c(x)$ by

$$F_d(x) := \frac{1}{2\pi} h \sum_{j=0}^{N-1} e^{-i\mathbf{u}_j x} \phi_r(\mathbf{u}_j). \tag{15}$$

Assume (2) holds, then $|\phi(u + iy)| \leq E(e^{-yX}) < \infty$ also holds for any $y \in (a^-, a^+)$. From Theorem 6.6 in Feng and Linetsky (2008), the discretization error is bounded by

$$|F_c(x) - F_d(x)| \leq A \frac{e^{-2\pi\alpha/h}}{2\pi(1 - e^{-2\pi\alpha/h})}, \tag{16}$$

where $\alpha > 0$ is such that $[-\alpha, \alpha] \subset (a^-, a^+)$, if the Fourier transform ϕ_r is absolutely integrable, $\int_{-\alpha}^{\alpha} |\phi_r(u + iy)| dy \to 0$ as $|u| \to \infty$ and

$$A := e^{\alpha x} \int_{\mathbb{R}} |\phi_r(u + i\alpha)| du + e^{-\alpha x} \int_{\mathbb{R}} |\phi_r(u - i\alpha)| du$$

is finite. Further, from (6), the following holds for $|x| \leq D/2$

$$\begin{aligned} A &= \int_{\mathbb{R}} \frac{e^{-D\alpha} |e^{2D\alpha} - 2e^{D\alpha} \cos(uD) + 1|}{2\sqrt{u^2 + \alpha^2}} \left(e^{\alpha x} |\phi(u + i\alpha)| + e^{-\alpha x} |\phi(u - i\alpha)| \right) du \\ &\leq \frac{1}{2\alpha} e^{-D\alpha/2} (e^{D\alpha} + 1)^2 \int_{\mathbb{R}} \left(|\phi(u + i\alpha)| + |\phi(u - i\alpha)| \right) du, \end{aligned} \tag{17}$$

where we have used $|e^{2D\alpha} - 2e^{D\alpha} \cos(uD) + 1| / \sqrt{u^2 + \alpha^2} \leq (e^{D\alpha} + 1)^2 / \alpha$.

3 The CGMY process

A CGMY process $X(t)$, $t \geq 0$ on a probability space $(\Omega, \mathcal{F}, \mathbb{P})$ is a pure jump process with Lévy density

$$\nu_X(x) := C\left(\frac{e^{-G|x|}}{|x|^{1+Y}} 1_{x<0} + \frac{e^{-Mx}}{x^{1+Y}} 1_{x>0}\right), \tag{18}$$

parameters $C > 0$, $G \geq 0$, $M \geq 0$, $Y < 2$, and characteristic function

$$E\left(e^{iuX(t)}\right) = \exp\left(tC\Gamma(-Y)\left((G+iu)^Y - G^Y + (M-iu)^Y - M^Y\right)\right). \tag{19}$$

It follows by differentiation of the characteristic exponent that the first four cumulants of the CGMY process are

$$\begin{aligned}
c_1(X(t)) &:= E(X(t)) = C\Gamma(1-Y)\left(M^{Y-1} - G^{Y-1}\right)t, \\
c_2(X(t)) &:= \mathrm{Var}(X(t)) = C\Gamma(2-Y)\left(M^{Y-2} + G^{Y-2}\right)t, \\
c_3(X(t)) &:= E\left((X(t) - E(X(t)))^3\right) = C\Gamma(3-Y)\left(M^{Y-3} - G^{Y-3}\right)t, \\
c_4(X(t)) &:= E\left((X(t) - E(X(t)))^4\right) - 3\mathrm{Var}(X(t))^2 = C\Gamma(4-Y)\left(M^{Y-4} + G^{Y-4}\right)t.
\end{aligned}$$

Consequently, the process has positive (resp. negative) skewness if $G > M$ (resp. $G < M$); further, the process is leptokurtic and the excess kurtosis is controlled by the parameter C.

The parameter Y characterizes the fine structure of the jumps of the CGMY process (see Carr et al., 2002). In details, for $Y < 0$ the process exhibits finite activity (i.e., the process has a finite number of jumps in any finite time period). In this case, CGMY can be considered as a compound Poisson process with arrival rate $C\Gamma(-Y)\left(G^Y + M^Y\right)$ and jump size which follows an asymmetric double gamma distribution with density

$$\begin{aligned}
&p\frac{G^{-Y}}{\Gamma(-Y)} e^{Gx}(-x)^{-1-Y} 1_{x<0} + q\frac{M^{-Y}}{\Gamma(-Y)} e^{-Mx} x^{-1-Y} 1_{x>0}; \\
&p := \frac{G^Y}{G^Y + M^Y}, \qquad q := 1 - p.
\end{aligned}$$

For $Y \in (0,1)$ the process has trajectories of infinite activity and finite variation (in other words, relative calmness is observed between big jumps), whilst for $Y \in (1,2)$ the process has infinite variation (there is a high degree of activity near zero as many small oscillations are observed between big jumps).

As shown by Madan and Yor (2008), the CGMY process can be represented as a subordinated Brownian motion

$$X(t) = \theta Z(t) + W(Z(t)),$$

where $Z(t)$ is a subordinator independent of the Brownian motion $W(t)$ with

$$E\left(e^{-\mu Z(t)}\right) = \exp(tC\Gamma(-Y)(2(2\mu + GM)^{\frac{Y}{2}}\cos(\zeta(\mu; G, M)Y) - M^Y - G^Y)), \tag{20}$$

for a complex number μ, $\zeta(\mu; G, M) := \arctan(\sqrt{2\mu - \theta^2}/\tilde{\theta})$, $\theta := (G - M)/2$ and $\tilde{\theta} := (G + M)/2$. For $Y > 0$ the subordinator Z is absolutely continuous with respect to the one-sided $Y/2$-stable subordinator and has Lévy density

$$\nu_Z(z) := s(z)\,\nu_0(z), \tag{21}$$

where

$$s(z) := \frac{\Gamma(Y)}{\Gamma(Y/2)\,2^{Y/2-1}} e^{\frac{z}{2}(\theta^2 - \tilde{\theta}^2)} h_{-Y}\left(\tilde{\theta}\sqrt{z}\right),$$

$h_v(x)$ is the Hermite function with parameter v and

$$\nu_0(z) := C\frac{2^{-Y/2}\sqrt{\pi}}{\Gamma(Y/2 + 1/2)}\frac{1}{z^{Y/2+1}}.$$

4 Monte Carlo simulation with Fourier transform

Monte Carlo methods rely on the inversion of the relevant distribution function. This generally applies to the increments of the actual process or, in case of subordinated Brownian motions such as the VG or the NIG, its subordinator (e.g., see Cont and Tankov, 2004, and

references therein). However, the distribution functions of the CGMY process and its subordinator are unknown; hence, in the following we show how to adapt the transform inversion discussed in Section 2 to recover the distributions of interest up to a pre-specified degree of accuracy. We note at this stage that, when applied to the CGMY process, this method allows for two different implementations. On the one hand, we can sample directly from the CGMY distribution using the characteristic function (19) (implementation MC-FT1). Alternatively, as the CGMY process is a subordinated Brownian motion, we can first sample from the distribution of the subordinator using (20) and then combine with sample increments of the Brownian motion (implementation MC-FT2).

4.1 Error bounds for the CDF Fourier inversion formula

4.1.1 The case of the CGMY process

Let $X(t)$ be the CGMY process. In the following theorem, we derive an explicit expression for the absolute value of the characteristic function of the CGMY process which allows us to study the effect of values of the parameter Y in the ranges $(-\infty, 0)$, $(0, 1)$, $(1, 2)$ on its tail behaviour. Depending on this, we then derive explicit bounds for the absolute value of the characteristic function for use in transform inversion.

Theorem 1 *Let $\phi_X(u;t)$, $u \in \mathbb{R}$, be the characteristic function of the process $X(t)$ given by (19). The following statements hold.*

(i) The absolute value $|\phi_X(u;t)|$ is given by

$$|\phi_X(u;t)| = e^{tK+tC|u|^Y f(u)}, \tag{22}$$

where

$$f(u) := \Gamma(-Y)\left[\left(\frac{G^2}{u^2}+1\right)^{Y/2}\cos\left(Y\arctan\frac{u}{G}\right)+\left(\frac{M^2}{u^2}+1\right)^{Y/2}\cos\left(Y\arctan\frac{u}{M}\right)\right] \tag{23}$$

and $K := -C\Gamma(-Y)(M^Y + G^Y)$ *is a constant.*

(ii) The function $f(u)$ *given by (23) is even, negative, and*

(a) monotone increasing for $u > 0$ *when* $Y \in (0, 1)$*;*

(b) monotone decreasing for $u > u^*$ *when* $Y \in (1, 2)$*, where*

$u^* := \max(G, M) \max[\tan(\pi/(2Y)),\ -1/\tan(Y\pi/2)] > 0.$

(iii) The absolute value $|\phi_X(u; t)|$ *is bounded by*

$$|\phi_X(u; t)| \leq e^{tK - b|u|^Y} \tag{24}$$

(a) for $u \in \mathbb{R}$ *and* $Y \in (0, 1)$ *with* $b := -t2C\Gamma(-Y)\cos(\pi Y/2) > 0$*;*

(b) for $|u| > u^*$ *and* $Y \in (1, 2)$ *with* $b := -tCf(u^*) > 0$*.*

Proof. See Appendix A.1. ■

Expression (24) provides us with an analytic bound for the characteristic function of the CGMY process that exhibits exponential decay. Therefore, the exponential tail condition (11) holds with

$$B = e^{tK},\ b = -t2C\Gamma(-Y)\cos(\pi Y/2) > 0,\ \beta = Y \text{ for } u \in \mathbb{R},\ Y \in (0, 1); \tag{25}$$

$$B = e^{tK},\ b = -tCf(u^*) > 0,\ \beta = Y \text{ for } |u| > u^*,\ Y \in (1, 2). \tag{26}$$

For $Y \in (1, 2)$ an exponential bound of the form (24) is not possible to derive for $u \in \mathbb{R}$ as function $f(u)$ in (23) increases unbounded as u goes to zero. However, as shown in Theorem 1, this limitation can be bypassed by truncating the range of values u. In addition, it is shown in Appendix B that for $Y > 0$ the CGMY process is selfdecomposable, hence the more conservative condition (13) can be considered, if necessary, with $u \in \mathbb{R}$ and parameters $\beta \in (1, \infty)$ and $B = \max_{u>0} |\phi_X(u; t)u^\beta|$.

For $Y < 0$, $\lim_{|u|\to\infty} |\phi_X(u; t)| = e^{tK} > 0$, therefore $\phi_X(u; t)$ is not absolutely integrable and condition (7) is not satisfied. Note also that the integral (10) defining the truncation

error is not convergent. This precludes retrieving the distribution function by inversion of the characteristic function and the use of the simulation method described in Sections 4.2–4.3. Nevertheless, this method is of less interest when $Y < 0$ since in this case the CGMY process is of compound Poisson type with known law of increments (see Section 3) whose sample paths can be simulated exactly using standard techniques (e.g., see Cont and Tankov, 2004).

The upper bounds of the regularization error (5) and discretization error (16) depend on the positive parameter α so that $[-\alpha, \alpha] \subset (a^-, a^+)$ with $|\phi_X(u+iy;t)| \leq E(e^{-yX(t)}) < \infty$ for $y \in (a^-, a^+)$. From (19) we have

$$\begin{aligned} \phi_X(u+iy;t) &= \exp\left(tC\Gamma(-Y)((G-y+iu)^Y - G^Y + (M+y-iu)^Y - M^Y)\right) \\ &=: \xi_y \phi_{X_y}(u;t), \end{aligned} \tag{27}$$

where $\xi_y := \exp\left(-tC\Gamma(-Y)(G^Y - G_y^Y + M^Y - M_y^Y)\right)$ is a constant, and ϕ_{X_y} denotes the characteristic function of the CGMY process $X_y(t)$ with parameters C, Y, $G_y := G - y > 0$, $M_y := M + y > 0$. To ensure G_y, M_y are positive, we require that $y \in (-M, G)$ implying $0 < \alpha < \min(G, M)$. In addition, from (17) and (27), we have

$$A \leq \frac{1}{\alpha} e^{-D\alpha/2}(e^{D\alpha}+1)^2 \left(\xi_\alpha \int_0^\infty |\phi_{X_\alpha}(u;t)|du + \xi_{-\alpha} \int_0^\infty |\phi_{X_{-\alpha}}(u;t)|du\right), \tag{28}$$

where $|\phi_{X_{\pm\alpha}}(u;t)|$ is given by (22) for the indicated parameters. In the case $Y \in (0,1)$ we further have from (24)

$$A \leq \frac{2}{\alpha} e^{-D\alpha/2}(e^{D\alpha}+1)^2 B \int_0^\infty e^{-bu^\beta} du = \frac{2e^{-D\alpha/2}(e^{D\alpha}+1)^2 B\Gamma(1/\beta)}{\alpha\beta b^{1/\beta}}, \tag{29}$$

where B, b, β are given by (25).

4.1.2 The case of the CGMY subordinator

Let $Z(t)$ be the subordinator of the CGMY process. The next theorem studies the absolute value of the characteristic function of $Z(t)$ for use on recovering the associated distribution

function by transform inversion. Similarly to the case of the CGMY process, its tail behaviour is affected by the choice of values of $Y \in (0,1) \cup (1,2)$.

Theorem 2 *Let $\phi_Z(u;t)$ be the characteristic function of the subordinator $Z(t)$ given by (20) for $\mu = iu$, where $u \in \mathbb{R}$. Let $K = -C\Gamma(-Y)(M^Y + G^Y)$ and suppose $G \neq M$. The following statements hold.*

(i) The absolute value $|\phi_Z(u;t)|$ is given by

$$|\phi_Z(u;t)| = e^{tK + tC|u|^{Y/2} f(u)}, \ u \in \mathbb{R}, \tag{30}$$

where

$$\begin{aligned}
f(u) &:= 2\Gamma(-Y)\left(\frac{G^2M^2}{u^2} + 4\right)^{Y/4} \left[\cos\left(\frac{Y}{2}\arctan\frac{2u}{GM}\right)\cos(Ya(u))\cosh(Yb(u))\right. \\
&\quad \left. + \sin\left(\frac{Y}{2}\arctan\frac{2u}{GM}\right)\sin(Ya(u))\sinh(Yb(u))\right], \qquad (31)\\
a(u) &:= \frac{\pi}{4} - \frac{1}{2}\arctan\left(\frac{1 - x(u)^2 - y(u)^2}{2x(u)}\right), \ a(0) = 0, \qquad (32)\\
b(u) &:= \frac{1}{4}\ln\left(\frac{x(u)^2 + (y(u)+1)^2}{x(u)^2 + (y(u)-1)^2}\right), \ b(0) = \ln\sqrt{\frac{G}{M}}, \qquad (33)\\
x(u) &:= \tilde{\theta}^{-1}(\theta^4 + 4u^2)^{1/4}\cos\left(-\frac{1}{2}\arctan(2\theta^{-2}u) + \frac{\pi}{2}1_{u\geq 0} - \frac{\pi}{2}1_{u<0}\right), \qquad (34)\\
y(u) &:= \tilde{\theta}^{-1}(\theta^4 + 4u^2)^{1/4}\sin\left(-\frac{1}{2}\arctan(2\theta^{-2}u) + \frac{\pi}{2}1_{u\geq 0} - \frac{\pi}{2}1_{u<0}\right). \qquad (35)
\end{aligned}$$

(ii) The function $f(u)$ given by (31) is even and, for $Y \in (0,1)$,

(a) $f(u) < 0, f'(u) > 0$ for $u > 0$ when $|\theta/\tilde{\theta}| > 1/\sqrt{3}$;

(b) $f(u) < 0, f'(u) > 0$ for $u > u^* > 0$, where u^* satisfies

$$\tan\left(\frac{1}{2}\arctan(2\theta^{-2}u^*)\right) = \tanh\left(\frac{1}{2}\text{arcosh}(\tilde{\theta}^2/\theta^2 - 2)\right), \tag{36}$$

when $|\theta/\tilde{\theta}| \leq 1/\sqrt{3}$.

(iii) For $Y \in (0,1)$, the absolute value $|\phi_Z(u;t)|$ is bounded by

$$|\phi_Z(u;t)| \leq e^{tK + t2C\Gamma(-Y)2^{Y/2}\cos(\pi Y/4)\cos(\pi Y/2)|u|^{Y/2}} \tag{37}$$

for $u \in \mathbb{R}$, if $|\theta/\tilde{\theta}| > 1/\sqrt{3}$; for $|u| > u^*$, if $|\theta/\tilde{\theta}| \leq 1/\sqrt{3}$, where u^* satisfies (36).

Proof. See Appendix A.2. ■

Given the conditions derived in Theorem 2, for $Y \in (0,1)$ we have from (37) that

$$B = e^{tK}, b = -t2C\Gamma(-Y)2^{Y/2}\cos(\pi Y/4)\cos(\pi Y/2) > 0 \text{ and } \beta = Y/2. \tag{38}$$

For $Y \in (1,2)$ the function $f(u)$ given by (31) is unbounded as u approaches zero. We have not been able to prove sufficient monotonicity conditions for a valid finite upper bound to $f(u)$, and consequently a bound of the form (11) for the absolute value of the characteristic function, even for a truncated range of values u. Still, the subordinator is selfdecomposable (see Appendix B) satisfying (13), which can be used as an alternative, with $\beta \in (1,\infty)$ and $B = \max_{u>0} |\phi_Z(u;t)u^\beta|$.

To obtain the upper bounds of the regularization error (5) and discretization error (16), consider

$$\begin{aligned} \phi_Z(u+iy;t) &= \exp\left(tC\Gamma(-Y)(2(-2iu + GM + 2y)^{Y/2}\cos(Y\zeta(-iu+y;G,M)) - M^Y - G^Y)\right) \\ &=: \xi_y \phi_{Z_y}(u;t), \end{aligned} \tag{39}$$

where ϕ_{Z_y} denotes the characteristic function of the CGMY subordinator $Z_y(t)$ with parameters C, Y,

$$\begin{aligned} G_y &:= \frac{M_y}{2(GM+2y)}\left(\sqrt{(G-M)^2 - 8y}(G+M) - 4y + G^2 + M^2\right), \\ M_y &:= \frac{\sqrt{2}}{2}\sqrt{-\sqrt{(G-M)^2 - 8y}(G+M) - 4y + G^2 + M^2} \end{aligned}$$

with $y \in (-GM/2, (G-M)^2/8)$, so that conditions

$$\begin{aligned} G_y M_y &= GM + 2y > 0, \\ (G_y - M_y)^2 &= (G-M)^2 - 8y > 0, \\ G_y + M_y &= G + M, \\ G_y &> 0, M_y > 0 \end{aligned}$$

are satisfied. Then, $0 < \alpha < \min(GM/2, (G-M)^2/8)$ so that $[-\alpha, \alpha] \subset (-GM/2, (G-M)^2/8)$. From (17) and (39) we obtain

$$A \leq \frac{1}{\alpha} e^{-D\alpha/2}(e^{D\alpha}+1)^2 \left(\xi_\alpha \int_0^\infty |\phi_{Z_\alpha}(u;t)| du + \xi_{-\alpha} \int_0^\infty |\phi_{Z_{-\alpha}}(u;t)| du \right), \tag{40}$$

where $|\phi_{Z_{\pm\alpha}}(u;t)|$ follows from (30) for the indicated parameters. If $Y \in (0,1)$ and $|G_{\pm\alpha} - M_{\pm\alpha}|/(G_{\pm\alpha} + M_{\pm\alpha}) > 1/\sqrt{3}$, we further have from (37)

$$A \leq \frac{2}{\alpha} e^{-D\alpha/2}(e^{D\alpha}+1)^2 B \int_0^\infty e^{-bu^\beta} du = \frac{2e^{-D\alpha/2}(e^{D\alpha}+1)^2 B \Gamma(1/\beta)}{\alpha\beta b^{1/\beta}}, \tag{41}$$

where B, b, β are given by (38).

4.2 Evaluating the CDF by numerical transform inversion

Following our earlier discussion, we identify three sources of error when using F_d in (15) to approximate the required CDF, F: the regularization, truncation and discretization errors. Given our upper bounds for these errors, we are able to constrain them within pre-specified tolerance levels and compute the CDF numerically at the desired accuracy. Suppose (without loss of generality) that each error term contributes equally to the total approximation error, for which we assume a target level $\epsilon > 0$.

4.2.1 Regularization error

From (3)–(5) the tail probabilities and the regularization error are exponentially decreasing functions of parameter $D > 0$ which determines the truncation of the domain of the CDF from $\mathbb{R}$ to $[-D/2, D/2]$. The error also depends on parameter α. Based on (3)–(4), we use standard root finding procedure to find the smallest value of D which satisfies $1 - F(D/2) < \epsilon/3$, $F(-D/2) < \epsilon/3$, subject to $0 < \alpha < \min(G, M)$ for the CGMY process and $0 < \alpha < \min(GM/2, (G-M)^2/8)$ for the subordinator. The regularization error given by (5) is then guaranteed to be bounded by $\epsilon/3$.

4.2.2 Truncation error

To bound the truncation error (12) above by $\epsilon/3$, in addition to our earlier choice for D, we consider fixed parameters B, b, β given explicitly by (25)–(26) for the CGMY for different ranges of the process parameter Y. Then, by employing a root finding procedure, we determine L from (12), i.e., the bounded domain $[-L/2, L/2]$ of the Fourier transform of the regularized CDF (6). Note that for $Y \in (1, 2)$ we need to ensure that $L > 2\lceil u^* \rceil$ holds (see 26), where $u^* = \max(G, M) \max[\tan(\pi/(2Y)), -\tan^{-1}(Y\pi/2)]$ and $\lceil u^* \rceil$ denotes the nearest integer greater than u^*. The corresponding parameters B, b, β for the CGMY subordinator are given by (38) for $Y \in (0, 1)$. Note in this case that for $|G - M|/(G + M) \leq 1/\sqrt{3}$ we need to choose $L > 2\lceil u^* \rceil$, where u^* satisfies Eq. (36). In the absence of a bound of the form (12) when $Y \in (1, 2)$ (see discussion in Section 4.1.2), we resort to (14) from which we compute $L = 2[\epsilon\pi(\beta - 1)/(3DB)]^{1/(1-\beta)}$ with $\beta \in (1, \infty)$ and $B = \max_{u>0} |\phi_Z(u; t)u^\beta|$ which can be found numerically given the explicit expression (30) for $|\phi_Z(u; t)|$.

4.2.3 Discretization error

Given parameters D, α, B, b, β, we can then compute parameter A of the discretization error bound (16). In particular, for $Y \in (0, 1)$, we have been able to obtain explicit upper bounds for A for both the CGMY process (see Eq. 29) and the CGMY subordinator (see Eq.

41). Alternatively, for $Y \in (0,1) \cup (1,2)$ one can obtain an estimate for A numerically based on (28) and (40) respectively for each model. Given A, we compute the grid spacing h for the truncated Fourier domain $[-L/2, L/2]$ so that the discretization error (16) is bounded above by $\epsilon/3$.

4.2.4 Transform inversion

Following the procedure described above, we obtain all the necessary parameters D, L, h for the numerical inversion of the Fourier transform (8) to recover the regularized CDF, and subsequently the CDF, subject to total target error ϵ. To this end, we select uniform grids $\mathbf{u} := \{(j - N/2)h\}_{j=0}^{N-1}$ and $\mathbf{x} := \{(l - N/2)\eta\}_{l=0}^{N-1}$ where $N := \lceil L/h \rceil$ and $\eta := D/N$. Denoting by $\mathbf{F}_d = \{F_d(\mathbf{x}_l)\}_{l=0}^{N-1}$ and $\varphi_r = \{\phi_r(\mathbf{u}_j)\}_{j=0}^{N-1}$ the values of F_d in (15) on grid $\mathbf{x}$ and ϕ_r in (6) on grid $\mathbf{u}$ respectively, we compute

$$\mathbf{F}_{d,l} = \frac{1}{2\pi} h \sum_{j=0}^{N-1} e^{-i\mathbf{u}_j \mathbf{x}_l} \varphi_{r,j} = \frac{1}{2\pi} h e^{-iu_0(\mathbf{x}_l - \mathbf{x}_0)} \sum_{j=0}^{N-1} e^{-ijlh\eta} e^{-i\mathbf{u}_j \mathbf{x}_0} \varphi_{r,j}. \tag{42}$$

Finally, we calculate the CDF as

$$\mathbf{F} \approx \mathbf{F}_r + \frac{\mathbf{1}}{\mathbf{2}} \approx \mathbf{F}_d + \frac{\mathbf{1}}{\mathbf{2}},$$

where $\frac{\mathbf{1}}{\mathbf{2}}$ is an N-dimensional vector of halves and $\mathbf{F} := \{F(\mathbf{x}_l)\}_{l=0}^{N-1}$ is the vector of approximate values of F on grid $\mathbf{x}$.

In (42), by setting $h\eta = LD/N^2 = 2\pi/N$, one obtains the usual discrete Fourier transform which can be computed fast on the grid $\mathbf{x}$ in $o(N \log_2 N)$ floating operations using the fast Fourier transform (FFT). For $h\eta = LD/N^2 = 2\pi\omega$ with arbitrary real $\omega \neq 1/N$, (42) generalizes to the so-called fractional discrete Fourier transform, which allows the user to bypass the undesirable restriction $LD = 2\pi N$. For this reason, we implement (42) using the fractional FFT which also provides us with multiple values of the distribution function simultaneously.

It is worth noting that the (absolute value) characteristic function bounds presented in Theorems 1 and 2 can be used in alternative methods for evaluating numerically the CDF based on characteristic function inversion, including, for example, the Hilbert transform method (see Feng and Linetsky, 2008; Chen et al., 2012) or (inverse) Laplace transform algorithms (e.g., see Cai et al., 2013).

4.3 Monte Carlo simulation

Assume $m > 0$ simulation trials and $n > 0$ time steps. The MC-FT1 algorithm proceeds as follows.

1. Compute (42) using the CGMY characteristic function given by (19). Compute $\mathbf{F}$ and store $(\mathbf{x}, \mathbf{F})$ to use for all m, n. Recall that the values of grid $\mathbf{x}$ represent the CGMY process increments which are stationary and independent. This allows us to compute and tabulate the distribution function once for use in all time steps and simulations. This is a substantial CPU power saving that is forgone when the method is applied to non-Lévy models (e.g., see Broadie and Kaya, 2006).

2. Generate matrix $\{U_{k,j}\}_{n\times m}$ where $U_{k,j} \sim \text{Unif}[0,1]$.

3. Use binary search to find $0 \leq l < N-1$ so that $\mathbf{F}_l \leq U_{k,j} < \mathbf{F}_{l+1}$ for $1 \leq k \leq n$ and $1 \leq j \leq m$. Use the uniform random samples on $[0,1]$ to generate samples $\hat{\mathbf{x}} := \{\hat{x}_{k,j}\}_{n\times m}$ from the CGMY distribution $F_{X(t)}$ by interpolating linearly between the tabulated values $(\mathbf{x}, \mathbf{F})$. The error of linear interpolation is $o(\eta^2)$. If $0 \leq U_{k,j} < \mathbf{F}_0$ and/or $\mathbf{F}_{N-1} \leq U_{k,j} < 1$, return respectively $\mathbf{x}_0$ and $\mathbf{x}_{N-1}$ (see Glasserman and Liu, 2010); the likelihood of these events is user-specified since $P(U_{k,j} < \mathbf{F}_0) = \mathbf{F}_0 < \epsilon/3$ and $P(U_{k,j} \geq \mathbf{F}_{N-1}) = 1 - \mathbf{F}_{N-1} < \epsilon/3$ (see Section 4.2.1), hence the error from using

such a convention is negligible. Based on the above, $F^{-1}_{X(t)}(U_{k,j}) \approx \hat{x}_{k,j}$ where

$$\hat{x}_{k,j} = \begin{cases} \mathbf{x}_0, & \text{if } U_{k,j} < \mathbf{F}_0 \\ \frac{U_{k,j}\eta + \mathbf{x}_l\mathbf{F}_{l+1} - \mathbf{x}_{l+1}\mathbf{F}_l}{\mathbf{F}_{l+1} - \mathbf{F}_l}, & \text{if } \mathbf{F}_l \leq U_{k,j} < \mathbf{F}_{l+1} \text{ for } 0 \leq l < N-1 \\ \mathbf{x}_{N-1}, & \text{if } U_{k,j} \geq \mathbf{F}_{N-1} \end{cases} .$$

Utilizing linear interpolation also ensures that $F_{X(t)}$ (and $F^{-1}_{X(t)}$) is monotonically increasing between grid points, providing that $\mathbf{F}_{l+1} > \mathbf{F}_l$ for all l; if strict monotonicity of $\{\mathbf{F}_l\}_{l=0}^{N-1}$ is violated, we increase the accuracy of the inversion scheme.

MC-FT2 proceeds along the same steps described above with the following modifications.

1. Replace the CGMY characteristic function with the one of the subordinator given by (20) with $\mu \in i\mathbb{R}$.

3. Generate samples $\hat{\mathbf{z}} := \{\hat{z}_{k,j}\}_{n\times m}$ from the subordinator's distribution $F_{Z(t)}$. Let $\hat{\mathbf{y}} := \{\hat{y}_{k,j}\}_{n\times m}$ where $\hat{y}_{k,j} \sim \mathcal{N}(0,1)$. Then $\hat{x}_{k,j} = \theta\hat{z}_{k,j} + \sqrt{\hat{z}_{k,j}}\hat{y}_{k,j}$.

5 Numerical study

For the purpose of implementing the MC-FT procedures in Sections 4.2–4.3, in what follows we compute sufficient grid parameter values to calculate numerically the CDFs of the CGMY process and the CGMY subordinator to achieve desired error tolerance, as described in Section 4.2. We then test the performance of MC-FT against the existing CGMY Monte Carlo methods on pricing different types of option contracts. We use the same parameters as in Poirot and Tankov (2006), hence we choose $C = 0.5$, $G = 2.0$, $M = 3.5$, $Y = 0.5$ (set I), i.e., CGMY with jumps of infinite activity and finite variation; and $C = 0.1$, $G = 2.0$, $M = 3.5$, $Y = 1.5$ (set II), i.e., CGMY with jumps of infinite variation.

5.1 Numerical CDFs

Table I provides the grid sizes D, L and the number of grid points N that need to be used in the Fourier inversion formula (42) for the CDF of the CGMY process $X(t)$ and the subordinator $Z(t)$ to ensure that the total approximation error (regularization, truncation of the state and Fourier domains, discretization) is bounded above by $\epsilon = 10^{-3}, \ldots, 10^{-10}, 10^{-13}$. The grid parameters are determined using our computable error bounds, following the procedure in Section 4.2 for each tolerance level, and are reported for $X(t)$, $t = 1, 1/12, 1/52$, and $Z(t)$, $t = 1$, for model parameters sets I and II, as required for our simulation experiments in Section 5.2. Given t, it can be seen that increasing precision results to larger parameters D, L controlling the regularization and truncation errors; the number of grid points N adjusts accordingly to offset the increase in the discretization error. It is also shown that the grid size L and, consequently, the number of grid points N increases with decreasing t and/or parameter Y. This is not surprising given the detrimental effect decreasing t and/or Y have on the decay of the absolute characteristic function value as shown in (24). We note the higher grid requirement in the case of the CGMY subordinator, especially for parameters set I; this is due to the slower decay of the corresponding characteristic function as $o(\exp(-b|u|^{Y/2}))$ (see 37), as opposed to $o(\exp(-b|u|^{Y}))$ (see 24) in the case of CGMY.

Additional numerical experiments for alternative model parameters $C = 2$, $G = 5$, $M = 15$, $Y = 0.5$ and $t = 0.5$, as assumed in Cai et al. (2013), have shown that selecting $D = 7.1$, $L = 149$, $N = 2^9$ based on the procedure in Section 4.2 suffice to compute using (42) $F_{X(0.5)}(-3.099) = 0.000000152486$, $F_{X(0.5)}(-0.029) = 0.450226233660$, $F_{X(0.5)}(1.506) = 0.999999976408$; our results are consistent with those obtained using the Laplace transform algorithm of Cai et al. (2013) and the Hilbert transform method of Chen et al. (2012) to 12 decimal places.

5.2 Pricing option contracts

The CGMY stock price process is given by

$$S(t) = S(0)\, e^{(r-q+\varpi)t+X(t)},\ 0 < t \leq T,$$

for given $S(0) > 0$, where $r > 0$ is the constant continuously compounded interest rate, $q > 0$ is the dividend yield, and the constant ϖ is chosen so that the discounted price process of the (tradable) asset is a martingale under some risk neutral measure $\mathbb{P}$, i.e.,

$$\varpi = -C\Gamma(-Y)\left((G+1)^Y - G^Y + (M-1)^Y - M^Y\right).$$

We further require $M \geq 1$ in order to ensure that $E^{\mathbb{P}}(e^{X(t)}) < \infty$. Finally, we consider a partition of the contingent claim lifetime $[0,T]$ $0 = t_0 < t_1 < ... < t_k < ... < t_n = T$, with $t_k = t_0 + k\delta$ and $\delta := T/n$.

In order to assess the performance of the MC-FT scheme, we consider a European plain vanilla put option with terminal payoff

$$\pi(T) = (K - S(T))^+, \tag{43}$$

where K is the strike price; an Asian call option with discrete monitoring at dates $0 = t_0 < t_1 < ... < t_k < ... < t_n = T$ and payoff

$$\pi(T) = \left(\frac{1}{n+1}\sum_{k=0}^{n} S(t_k) - K\right)^+ \tag{44}$$

with fixed strike K; and a discretely monitored barrier call option of the type up-and-out (UOC) with payoff

$$\pi(T) = (S(T) - K)^+ 1_{\{\sup_{t\in\mathcal{T}} S(t) < B\}}, \tag{45}$$

where $\mathcal{T} := \{t_k\}_{k=0}^n$ and $B > S(0)$ is the barrier level. These options can be priced nu-

merically (without Monte Carlo) under the CGMY model at high precision using, for example, the Fourier-cosine series expansion of Fang and Oosterlee (2008) (payoff 43) and the backward convolution algorithms of Černý and Kyriakou (2011) (payoff 44) and Lord et al. (2008) (payoff 45). We use these methods to benchmark the proposed Monte Carlo scheme. Results are shown in Table II; the numerical CDFs used for the Monte Carlo experiment are obtained using the settings in Table I for $\epsilon = 10^{-10}$. The 95% confidence interval generated by the Monte Carlo simulation always contains the exact price produced by the benchmark algorithms.

Further, we compare the performance of MC-FT with the existing Monte Carlo methods of Poirot and Tankov (PT) (Poirot and Tankov, 2006), Madan and Yor (MY) (Madan and Yor, 2008), Baeumer and Meerschaert (AR) (Baeumer and Meerschaert, 2010) and Rosiński (SR) (Rosiński, 2007). In the interest of a fair comparison, all the schemes considered use programs coded on the same platform (MATLAB R2010b run on a Dell Optiplex 755 Intel Core 2 Duo PC 2.66GHz with 2.0GB RAM; the implementation of the MY scheme in MATLAB is based on the C++ code of Peter Tankov available at http://people.math.jussieu.fr/~tankov/). The PT scheme is considered only for the case of the European put option as it cannot be applied to generate the process path. Note that MY, AR and SR generate biased price estimators. In the MY approach, in fact, bias results from the truncation of the small jumps of the subordinator Z below some threshold level ε (see also Poirot and Tankov, 2006). In the AR sampling scheme, bias is originated by the truncation of the real line to the domain on which the tempering is performed (see Kawai and Masuda, 2011) and which is controlled by a parameter $\gamma > 0$, say. Note that the AR scheme is exact for $Y \in (0, 1)$ (i.e., set I). Finally, bias in the SR method is introduced by the truncation of the infinite summation representation of the CGMY process to a finite number of terms, say $\tilde{N}$. In the presence of bias, we measure the error of the Monte Carlo price estimates with the root mean square error RMSE $:= \sqrt{\text{bias}^2 + \sigma^2}$, where bias $:= \hat{\pi}_0 - \pi_0$, $\hat{\pi}_0$ is the price estimate calculated using 10^7 simulation trials, π_0 is the true price obtained by the benchmark methods and σ^2 is the sample variance. As MC-FT is implemented based on numerical CDF with error bounded

above by $\epsilon = 10^{-10}$, its approximation bias is negligible compared to the Monte Carlo simulation error itself. The PT scheme is also unbiased. Consequently, for both methods the RMSE coincides with the standard error.

A comparison in terms of speed and accuracy of the MC-FT schemes and the PT, MY and AR methods is illustrated in Figure 1, where we plot on a log-log scale the RMSE against the CPU time obtained for 10^4, 10^5, 10^6, 10^7 simulation trials when pricing the European put option with terminal payoff (43). The MY estimates are obtained using the threshold ε which originates an overall RMSE as close as possible to the one generated by the MC-FT schemes. This value depends on the parameter Y: for $Y = 0.5$ (set I) $\varepsilon = 10^{-4}$, while for $Y = 1.5$ (set II) $\varepsilon = 10^{-5}$. The parameter γ in the AR scheme for set II is chosen in a similar manner and fixed at 2. The steeper slopes in the plots indicate that both MC-FT1 and MC-FT2 outperform the other simulation approaches. More in details, MY and AR achieve same RMSE as MC-FT for the same number of simulation trials, quantified, for example, at 0.0197 (regardless of the parameters set used) when 10^6 trials are used. However, this is achieved at a higher CPU cost: under set I, for 10^6 trials MY uses 387 seconds to produce a price estimate, AR uses 446 seconds, whilst MC-FT1 and MC-FT2 require 0.56 seconds and 1.93 seconds respectively. Under set II, the CPU times are 1705, 2805, 0.47, 1.20 seconds for MY, AR, MC-FT1 and MC-FT2 respectively. The PT scheme, on the other hand, is the closest to the MC-FT implementations in terms of computing time, especially for a small number of simulation trials; however, both MC-FT1 and MC-FT2 prove to be more accurate generating smaller RMSE. For example, for the illustrative case of 10^6 trials, PT returns the option price in 0.81 seconds with a RMSE of 0.09.

Figure 1 also shows that MC-FT1 and MC-FT2 achieve the same accuracy for all simulation trials, however MC-FT1 is slightly faster. This is a consequence of the more time consuming CDF tabulation in MC-FT2 due to the larger number of grid points used in the numerical transform inversion to attain the desired error tolerance, as discussed in Section 5.1. As the number of simulation trials increases, the execution time of the simulation part overshadows the computational burden of CDF tabulation and the two MC-FT implemen-

tations converge.

If the SR method is used, the choice of the truncation threshold $\tilde{N}$ of the infinite series is an important issue to be addressed due to the trade-off between the approximation error and the CPU time, which is even more pronounced than in the MY and AR schemes. Our numerical exercise has shown that, for parameter $Y = 0.5$ (set I), SR with $\tilde{N} = 10^3$ produces same RMSE as the MC-FT schemes, however for higher computing time by a factor of 10^5. The efficiency gains provided by the MC-FT method are even more pronounced for $Y = 1.5$ (set II): the RMSE generated by the MC-FT schemes is smaller by a factor of 10^2 even when using SR with $\tilde{N} = 10^4$, whilst the saving in terms of CPU time is of a factor of 10^6. We have not explored higher values $\tilde{N}$ due to the large computing effort.

In light of the previous discussion, we present the results obtained only by the MC-FT1, MY and AR methods for the Asian option with payoff (44) and the UOC barrier option with payoff (45). Figures 2 and 3 illustrate the speed and accuracy of the methods for 10^6 simulation trials and quarterly, monthly and weekly monitoring (i.e., $n = 4, 12, 52$). The three simulation schemes achieve similar precision as measured by the RMSE, however at different computing costs. For illustration purposes, in the monthly monitoring case the Asian option price is generated with a RMSE of 0.019, whilst the UOC barrier option price estimate has a RMSE of 0.006, regardless of the parameters set used. The difference in CPU times, though, is significant: for both the Asian and UOC barrier options, MC-FT1 generates a price estimate in 7.4 seconds (set I) and 7 seconds (set II), MY requires instead 3828 seconds (set I) and 6309 seconds (set II), whilst AR requires 426 seconds (set I) and 1069 seconds (set II).

6 Extension to multivariate options

The proposed simulation methodology can be easily extended to accommodate multivariate option contracts. In this study we consider the case of a spread option with payoff function

$$\pi(T) = (S_2(T) - S_1(T) - K)^+$$

and an Asian basket option with terminal payoff

$$\pi(T) = \left(\frac{1}{d(n+1)} \sum_{j=1}^{d} \sum_{k=0}^{n} S_j(t_k) - K \right)^+, \tag{46}$$

where d denotes the number of assets in the portfolio. These are derivative contracts common in energy markets, where they trade OTC but also on commodity exchanges such as NYMEX (e.g., see Borovkova and Permana, 2010, and references therein).

The pricing of these contracts requires the construction of a multidimensional CGMY process with dependence between components. Recent contributions on multivariate Lévy processes include, amongst others, Ballotta and Bonfiglioli (2013) and Luciano and Semeraro (2010). In particular, Ballotta and Bonfiglioli (2013) use a two-factor approach in which each component of a d-dimensional Lévy process is given by the sum of an idiosyncratic and a systematic risk process. Convolution conditions are then imposed to guarantee that the given sum returns a process with known distribution in order to facilitate the calibration of the model. The construction proposed by Luciano and Semeraro (2010), instead, is specific to processes with known subordinated Brownian motion representation, such as the CGMY process, as dependence is induced by the subordinator, which is decomposed into an idiosyncratic and a systematic clock.

In this analysis we adopt the multivariate construction proposed by Ballotta and Bonfiglioli (2013) and use MC-FT1 to simulate CGMY variates directly which was shown above to be faster. More specifically, for $j = 1, \ldots, d$, let $L_j(t)$ and $L_{d+1}(t)$ be independent CGMY

processes with parameters $(C_{Lj}, G_{Lj}, M_{Lj}, Y)$ and (C_L, G_L, M_L, Y) respectively, representing the idiosyncratic and the systematic risk factors. Then, for $a_j \in \mathbb{R}$

$$\mathbf{X}(t) = (X_1(t), \ldots, X_d(t))^\top = (L_1(t) + a_1 L_{d+1}(t), \ldots, L_d(t) + a_d L_{d+1}(t))^\top \tag{47}$$

is a d-dimensional CGMY process, whose margins have parameters (C_j, G_j, M_j, Y) if the following convolution conditions are satisfied

$$\begin{cases} G_{Lj} = G_L/a_j, & j = 1, ..., d, \\ M_{Lj} = M_L/a_j, & j = 1, ..., d, \end{cases}$$

and $C_j = C_{Lj} + C_L a_j^Y$, $j = 1, ..., d$. Note that in this example we assume that all processes have the same parameter $Y < 2$, i.e., the same fine structure. The pairwise (linear) correlation coefficient is

$$\rho_{jl} := \mathrm{Corr}\left(X_j(t), X_l(t)\right) = a_j a_l \frac{\mathrm{Var}\left(L_{d+1}(1)\right)}{\sqrt{\mathrm{Var}\left(X_j(1)\right)\mathrm{Var}\left(X_l(1)\right)}}. \tag{48}$$

In order to adapt the MC-FT1 algorithm to the multivariate construction (47) for a d-dimensional problem, we require $(d+1)$ computations of the discrete transform (42) to evaluate the CDFs of the d idiosyncratic processes and the systematic component, each subject to error tolerance $\epsilon = 10^{-10}$. Similarly to the univariate case, these can be tabulated once at the beginning of the Monte Carlo simulation. The corresponding CGMY samples are generated using a cube of uniform random variates of dimension $n \times m \times (d+1)$ (see Section 4.3), and then combined under the linear transformation (47).

For the numerical test, we use the same data as in Ballotta and Bonfiglioli (2013), hence we calibrate the CGMY margins to market prices of vanilla options written on Ford Motor Company (F), Abbott Lab. (ABT), and Baxter Int. Inc. (BAX) as of September 2008. The parameters of the idiosyncratic and the systematic processes are obtained by fitting the correlation matrix and imposing the corresponding convolution conditions. As a proxy

for the correlation between $X_j(t), X_l(t)$, we consider the historical correlation estimated on a time window of 125 days up to (and including) the valuation date. All parameters are reported in Table III. The table also shows the accuracy with which the linear combination (47) reproduces the original market option data. In details, the table provides information on the error caused by fitting the correlation matrix (correlation fit error) and imposing convolution. Note that the convolution conditions are solved numerically originating an error, which we quantify by the difference between the first four cumulants of the CGMY margins and the linear combination (47) (cumulant error) and its impact on option prices (calibration error).

As spread options can be priced at high accuracy with transform techniques (e.g., see Lord et al., 2008), we can benchmark the multivariate MC-FT1 algorithm. For more accurate Monte Carlo price estimates, we further use antithetic variates (with the same total number of simulation trials as the crude MC-FT1). In this example, we assume spread options written on Ford (asset S_1) and Abbott (asset S_2). From Table IV, we observe that the reference prices lie in the 95% confidence interval generated by the MC-FT1 procedure.

MC-FT1 lends itself easily to more complicated multivariate contracts for which exact (non-Monte Carlo) pricing techniques are not currently available. To the best of our knowledge, this is the case, for example, with Asian basket options. By changing to the payoff (46), we use MC-FT1 to price Asian basket options written on Ford, Abbott and Baxter (asset S_3), see Table IV. Alternative pricing methods in the literature are based on the moment matching approach (e.g., see Borovkova and Permana, 2010, for an application in the traditional Gaussian economy); differently from the MC-FT sampling approach, though, the induced approximation error of the moment matching method is not directly quantifiable and therefore difficult to control.

7 Conclusions

In this paper, we present a Monte Carlo simulation method for the CGMY process based on sampling from CDF obtained by Fourier transform inversion. Based on the same principle, we study further the simulation of the CGMY using its Brownian subordination representation. We investigate sufficient conditions for the existence of explicit bounds for the error in transform inversion, which allow us to gauge the precision of the numerical CDF. The suggested sampling scheme is tested on numerical examples involving the pricing of single-asset plain vanilla and exotic options under a CGMY model of infinite activity with finite or infinite variation. The method provides access to the entire trajectory of the process and shows significant efficiency gain over other CGMY sampling schemes for different values of the process parameter $Y \in (0,1) \cup (1,2)$. Further, we extend to the multidimensional case by proposing a multivariate construction of the CGMY process and assessing the performance of the sampling scheme on pricing multi-names contracts.

Finally, we note that the MC-FT schemes, especially the MC-FT1 implementation, has the advantage of keeping the dimension of the problem at its minimal level; in this respect, the proposed approach is QMC friendly and further efficiency improvements can be expected by combining it with QMC/RQMC methods (see also Chen et al., 2012) for further considerations on the suitability of inverse transform methods for QMC implementations). The performance of QMC methods, though, depends also on the payoff function and the actual process construction (e.g., see Wang and Sloan, 2011, and references therein); the full investigation of these aspects for the case of the CGMY process and, more in general, other Lévy processes is left to future research.

A Proofs of Theorems

A.1 Proof of Theorem 1

Proof of (i). Define

$$\begin{aligned} w_1 &= G + iu \text{ with } \arg w_1 = \arctan\frac{u}{G},\ |w_1| = (G^2+u^2)^{1/2}, \\ w_2 &= M - iu \text{ with } \arg w_2 = -\arctan\frac{u}{M},\ |w_2| = (M^2+u^2)^{1/2}; \end{aligned}$$

therefore

$$w_j^Y = |w_j|^Y \left[\cos(Y \arg w_j) + i \sin(Y \arg w_j)\right]$$

for $j = 1, 2$. Then,

$$\phi_X(u;t) = \exp\left[tK + tC\Gamma(-Y)\left(w_1^Y + w_2^Y\right)\right]$$

from which result (22) follows. ■

Proof of (ii). As the cosine function is an even function, so is the function f, i.e., $f(-u) = f(u)$. Given this, in what follows we consider $u > 0$. Further,

$$\begin{aligned} f'(u) &= -Y\Gamma(-Y)\left[\left(\frac{G^2}{u^2}+1\right)^{Y/2}\frac{G}{G^2+u^2}\cos\left(Y\arctan\frac{u}{G}\right)\left(\frac{G}{u}+\tan\left(Y\arctan\frac{u}{G}\right)\right)\right. \\ &\quad \left. + \left(\frac{M^2}{u^2}+1\right)^{Y/2}\frac{M}{M^2+u^2}\cos\left(Y\arctan\frac{u}{M}\right)\left(\frac{M}{u}+\tan\left(Y\arctan\frac{u}{M}\right)\right)\right]. \end{aligned}$$

Note that $\cos(Y\arctan(u/G))$, $\cos(Y\arctan(u/M))$, $\tan(Y\arctan(u/G))$, and $\tan(Y\arctan(u/M))$ are: (a) positive when $Y \in (0,1)$ as $Y\arctan(u/G), Y\arctan(u/M) \in (0, Y\pi/2) \subset (0,\pi/2)$ for all $u > 0$; (b) guaranteed to be negative for $u > \max(G,M)\tan(\pi/(2Y)) > 0$ when $Y \in (1,2)$ as $Y\arctan(u/G), Y\arctan(u/M) \in (\pi/2, Y\pi/2) \subset (\pi/2,\pi)$. Consequently, under (a), function $f(u)$ is negative and monotone increasing for $u > 0$. Under (b), $f(u)$ is negative for $u > \max(G,M)\tan(\pi/(2Y))$; further, $f'(u)$ is negative if $|\tan(Y\arctan(u/G))| > G/u$,

and $|\tan(Y \arctan(u/M))| > M/u$, i.e., if $-\tan(Y\pi/2) > \max(G, M)/u$. Hence, both $f(u)$ and $f'(u)$ are negative for $u > \max(G, M) \max[\tan(\pi/(2Y)), -1/\tan(Y\pi/2)] = u^*$. ■

Proof of (iii). Consider case (a), hence $Y \in (0, 1)$. Then, it follows $f(0) \to -\infty$; further, $\lim_{u\to\infty} \cos(Y \arctan(u/G)) = \lim_{u\to\infty} \cos(Y \arctan(u/M)) = \cos(\pi Y/2)$ and $\lim_{u\to\infty} f(u) = 2\Gamma(-Y)\cos(\pi Y/2) < 0$. From part (ii), $f(u)$ is monotone increasing for $u > 0$; therefore, $f(u) \leq 2\Gamma(-Y)\cos(\pi Y/2)$. Since function f is even, the bound is also satisfied for $u < 0$. Consider case (b). Then, $0 > f(u^*) > f(u)$ as $f(u)$ is guaranteed to be negative and monotone decreasing for $u > u^*$ from part (ii). Since function f is even, the bound is also satisfied for $u < -u^*$. The proof is complete. ■

A.2 Proof of Theorem 2

Proof of (i). Define

$$\begin{aligned} w_1 &= 2iu - \theta^2 \text{ with } \arg w_1 = -\arctan(2\theta^{-2}u) + \pi 1_{u\geq 0} - \pi 1_{u<0}, \\ |w_1| &= (\theta^4 + 4u^2)^{1/2}, \end{aligned}$$

so that

$$w_1^{1/2} = |w_1|^{1/2} \left[\cos\left(\frac{1}{2}\arg w_1\right) + i \sin\left(\frac{1}{2}\arg w_1\right)\right].$$

Then,

$$\phi_Z(u; t) = \exp\left[tK + t2C\Gamma(-Y)(2iu + GM)^{Y/2} \cos(\zeta(iu; G, M)Y)\right],$$

where

$$\zeta(iu; G, M) = \arctan(\tilde{\theta}^{-1} w_1^{1/2}) \equiv \arctan(x(u) + iy(u)) \equiv a(u) + ib(u)$$

for real-valued functions $a(u), b(u), x(u), y(u)$ given by (32)–(35), see Abramowitz and Stegun (1968), p. 81. Note that $x(u) > 0$ when $u \neq 0$ and $x(0) = 0$, also $y(0) = \theta/\tilde{\theta} \in [-1, 1]$, hence

$a(0) = 0$ and $b(0) = \ln(\sqrt{G/M})$. The following also holds:

$$\cos(\zeta(iu; G, M)Y) = \cos(Ya(u))\cosh(Yb(u)) - i\sin(Ya(u))\sinh(Yb(u)).$$

Finally, define

$$w_2 = 2iu + GM \text{ with } \arg w_2 = \arctan\frac{2u}{GM}, \;\; |w_2| = (G^2M^2 + 4u^2)^{1/2},$$

so that

$$w_2^{Y/2} = |w_2|^{Y/2}\left[\cos\left(\frac{Y}{2}\arg w_2\right) + i\sin\left(\frac{Y}{2}\arg w_2\right)\right].$$

Then,

$$\phi_Z(u;t) = \exp\left[tK + t2C\Gamma(-Y)w_2^{Y/2}\cos\left(\arctan(\tilde{\theta}^{-1}w_1^{1/2})Y\right)\right]$$

from which result (30) follows by straightforward algebra. ■

A.2.1 Outline of proof of (ii)

We begin the path to proving part (ii) of Theorem 2 by establishing some useful results.

As the arctangent function is an odd function, $a(-u) = a(u)$ and $b(-u) = -b(u)$ which further imply that $f(-u) = f(u)$. Given this, in what follows we consider $u > 0$ only.

Define the ratio $\tau = \theta/\tilde{\theta} \in [-1, 1]$. For $u > 0$, let $\beta = \frac{1}{2}\arctan(2\theta^{-2}u) \in (0, \pi/4)$ so that $2u = \theta^2\tan(2\beta)$ and $\theta^4 + 4u^2 = \theta^4\sec^2(2\beta)$, then

$$x(u) = |\tau|\sin(\beta)\sqrt{\sec(2\beta)}, \;\; y(u) = |\tau|\cos(\beta)\sqrt{\sec(2\beta)}.$$

Further, let $\gamma = \tan\beta \in (0, 1)$, then $\cos\beta = 1/\sqrt{1+\gamma^2}$, $\cos(2\beta) = (1-\gamma^2)/(1+\gamma^2)$, $\tan(2\beta) = 2\gamma/(1-\gamma^2)$. Finally, consider the substitution $\gamma = \tanh v \in (0, 1)$ with $v \in (0, \infty)$, which yields

$$x(u) = |\tau|\sinh v, \;\; y(u) = |\tau|\cosh v.$$

This implies

$$\begin{aligned}\frac{x(u)^2+(y(u)+1)^2}{x(u)^2+(y(u)-1)^2} &= \frac{\tau^2\cosh(2v)+1+2|\tau|\cosh v}{\tau^2\cosh(2v)+1-2|\tau|\cosh v} =: R(v) \geq 1,\\ \frac{1-x^2(u)-y^2(u)}{2x(u)} &= \frac{1-\tau^2\cosh(2v)}{2|\tau|\sinh v} =: \alpha(v).\end{aligned}$$

Further

$$\frac{2u}{GM} = \frac{\tan(2\beta)}{\tau^{-2}-1} = \frac{2\gamma\tau^2}{(1-\gamma^2)(1-\tau^2)} = \frac{\tau^2\sinh(2v)}{1-\tau^2},$$

from which

$$\arctan\frac{2u}{GM} = \arctan\left(\frac{\tau^2\sinh(2v)}{1-\tau^2}\right) =: I(v).$$

Given the functions $R(v), \alpha(v), I(v)$, we define

$$g(v) = R(v)^{Y/4}\cos z_1(v) + R(v)^{-Y/4}\cos z_2(v), \tag{A.1}$$

where

$$\begin{aligned}z_1(v) &:= (I(v)-J(v))Y/2,\\ z_2(v) &:= (I(v)+J(v))Y/2,\\ J(v) &:= \pi/2 - \arctan\alpha(v).\end{aligned} \tag{A.2}$$

Using standard trigonometric identities and algebraic expressions of the sinh and cosh functions, we can rewrite function f in (31) as

$$f(u) = \Gamma(-Y)\left(\frac{G^2M^2}{u^2}+4\right)^{Y/4} g(v(u)),$$

where

$$v(u) = \operatorname{artanh}\left[\tan\left(\frac{1}{2}\arctan(2\theta^{-2}u)\right)\right] > 0 \tag{A.3}$$

for $u > 0$. Note that $v'(u) = (\theta^4 + 4u^2)^{-1/2} > 0$, hence $v(u)$ is an increasing, nonnegative function of u. Then,

$$f'(u) = \Gamma(-Y)\left(\frac{G^2M^2}{u^2} + 4\right)^{Y/4}\left[-\frac{Y}{2}\frac{G^2M^2}{u(G^2M^2+4u^2)}g(v) + g'(v)v'(u)\right], \tag{A.4}$$

where

$$\begin{aligned} g'(v)v'(u) &= \frac{Y}{2}v'(u)\left[\frac{R'(v)}{2R(v)}\left(R(v)^{Y/4}\cos z_1(v) - R(v)^{-Y/4}\cos z_2(v)\right)\right. \\ &\quad \left. -R(v)^{Y/4}(I'(v) - J'(v))\sin z_1(v) - R(v)^{-Y/4}(I'(v) + J'(v))\sin z_2(v)\right] \end{aligned} \tag{A.5}$$

In what follows, we derive sufficient conditions to ensure that function g is positive with g' negative, hence function f is negative and f' is positive for $Y \in (0,1)$. To this end, we study first the behaviour of functions I, J and R.

The behaviour of functions I and J. From the definitions it follows that

$$I'(v) = \frac{2\tau^2(1-\tau^2)\cosh(2v)}{1 - 2\tau^2 + \tau^4\cosh^2(2v)},\ J'(v) = \frac{2|\tau|\cosh(v)(1 + \tau^2(\cosh(2v) - 2))}{1 - 2\tau^2 + \tau^4\cosh^2(2v)}. \tag{A.6}$$

We notice from (A.6) that the derivatives I', J' share the same denominator, which is positive, and that their numerators are also positive. Further, as $I(0) = J(0) = 0$, I, J are increasing, nonnegative functions. Consider the difference $I - J$. Using the identity $\cosh(2v) = 2\cosh^2 v - 1$ and the substitution $\delta = \cosh v \geq 1$, it follows that

$$I'(v) - J'(v) = -\frac{2|\tau|(\delta + |\tau|)}{1 - 2\tau^2 + \tau^4\cosh^2(2v)}G(\delta),$$

where $G(\delta) := 2\delta^2\tau^2 - 2\delta|\tau| + 1 - \tau^2$ has a minimum value at $\delta^* = 1/(2|\tau|) > 1$ for $|\tau| < 1/2$ equal to $G(\delta^*) = 1/2 - \tau^2 > 0$. If $|\tau| \geq 1/2$, the minimum is at $\delta^* = 1$ with $G(1) = (|\tau| - 1)^2 > 0$. Hence, $I'(v) - J'(v) < 0$. Since $\lim_{v\to\infty} I(v) = \pi/2$ and

$\lim_{v\to\infty} J(v) = \pi$, it follows that $I(v) - J(v)$ is monotone decreasing from 0 to $-\pi/2$. In addition, $I(v) + J(v)$ is monotone increasing from 0 to $3\pi/2$.

The behaviour of functions R and g. We have shown already that $R(v) \geq 1$ for $v > 0$. Further

$$\frac{R'(v)}{2R(v)} = \frac{2|\tau|\sinh(v)(1-\tau^2(2+\cosh(2v)))}{1-2\tau^2+\tau^4\cosh^2(2v)},$$

where the denominator in the last equality is positive. Consequently, $R'(v) < 0$: (a) for all $v > 0$ when $|\tau| > 1/\sqrt{3}$ since $1-\tau^2(2+\cosh(2v)) < 1-3\tau^2 < 0$; (b) for all values of v such that $\cosh(2v) > \tau^{-2} - 2 \geq 1$, i.e., for $v > v^* := \frac{1}{2}\text{arcosh}(\tau^{-2}-2) > 0$ where $|\tau| \leq 1/\sqrt{3}$.

We inspect the sign of the three terms in (A.5): firstly, $R \geq 1$, and $R' < 0$ under either condition (a) or (b). Recall further that $z_1 = (I-J)Y/2 \in (-Y\pi/4, 0) \subset (-\pi/2, 0)$ and $z_2 = (I+J)Y/2 \in (0, 3Y\pi/4) \subset (0, 3\pi/2)$ since $Y < 2$. If $|I-J|Y/2 < (I+J)Y/2 < \pi/2$, we have that $\cos z_1 > \cos z_2 > 0$, else if $|I-J|Y/2 < \pi/2 < (I+J)Y/2 < 3\pi/2$, we have that $\cos z_2 < 0$; in either case we conclude that

$$\frac{R'(v)}{2R(v)}\left(R(v)^{Y/4}\cos z_1(v) - R(v)^{-Y/4}\cos z_2(v)\right) < 0$$

for $v > 0$. Secondly, the term

$$R(v)^{Y/4}(I'(v) - J'(v))\sin z_1(v) > 0,$$

since $I' - J' < 0$ and $\sin z_1 < 0$. Finally, $I' + J' > 0$ and $\sin z_2 > 0$ since $z_2 = (I+J)Y/2 \in (0, 3Y\pi/4) \subset (0, \pi)$ if we restrict $Y < 4/3$, in which case the term

$$R(v)^{-Y/4}(I'(v) + J'(v))\sin z_2(v) > 0.$$

In summary, $g'(v)v(u) < 0$ when either condition (a) or (b) holds in addition to $Y < 4/3$.

We use our previous conclusion to determine the sign of function $g(v)$. We inspect

both conditions. Assume condition (a) holds: from (A.1), $g(0) = R(0)^{Y/4} + R(0)^{-Y/4} = [(|\tau|+1)^2/(|\tau|-1)^2]^{Y/4} + [(|\tau|-1)^2/(|\tau|+1)^2]^{Y/4} > 0$, and $\lim_{v\to\infty} g(v) = \lim_{v\to\infty} \cos z_1(v) + \lim_{v\to\infty} \cos z_2(v) = \cos(\pi Y/4) + \cos(3\pi Y/4) > 0$ if we restrict $Y < 1$. Since $g'(v) < 0$ for all $v > 0$, then $g(v) > 0$. Instead, suppose condition (b) holds: we need to examine the sign of $g(v^*)$. We have that $0 < J(v^*) < \pi/2$, which follows from (A.2) as $\alpha(v^*) = (1 - \tau^2 \cosh(2v^*)) / (2|\tau| \sinh v^*) = |\tau| / \sinh v^* > 0$ and $0 < \arctan \alpha(v^*) < \pi/2$. Also $0 < I(v^*) < \pi/2$, therefore $z_2(v^*) = (I(v^*) + J(v^*))Y/2 < \pi/2$ and $\cos z_2(v^*) > 0$ if we restrict $Y < 1$. Further, $\cos z_1(v^*) > 0$ and $R(v^*) > 0$, implying $g(v^*) > 0$. We conclude that $g(v) > 0$ for $v > v^*$ when $Y < 1$.

Proof of (ii). Based on the analysis in Section A.2.1, we conclude that $f'(u)$ in (A.4) is positive, i.e., $f(u)$ in (31) is monotone increasing, for $Y \in (0, 1)$ and (a) all $u > 0$ when $|\tau| > 1/\sqrt{3}$; (b) all values $u > u^* > 0$, where u^* satisfies $\tan\left(\frac{1}{2} \arctan(2\theta^{-2}u^*)\right) = \tanh(v^*)$ in virtue of (A.3) with $v^* = \frac{1}{2}\text{arcosh}(\tau^{-2} - 2) > 0$ when $|\tau| \leq 1/\sqrt{3}$. Under either condition (a) or (b), f is also negative. ■

Proof of (iii). Let $Y \in (0, 1)$. From (31), $f(0) \to -\infty$. Also $x(\infty) \to \infty$, $y(\infty) \to \infty$, implying $\lim_{u\to\infty} a(u) = \pi/2$, $\lim_{u\to\infty} b(u) = 0$; therefore $\lim_{u\to\infty} f(u) = 2\Gamma(-Y)2^{Y/2} \cos(\pi Y/4) \cos(\pi Y/2) < 0$. From part (ii), $f(u)$ is monotone increasing for $u > 0$ when $|\tau| > 1/\sqrt{3}$, and for $u > u^*$ when $|\tau| \leq 1/\sqrt{3}$. Hence, for values of u in the relevant ranges, we have that $f(u) \leq \lim_{u\to\infty} f(u)$. As function f is even, the bound is also satisfied for $u < 0$ or $u < -u^*$. This concludes the proof of the theorem. ■

B Selfdecomposability of the CGMY process and the CGMY subordinator

For the case of the CGMY process, consider its Lévy density given by (18). It follows that

$$k_X(x) = \nu_X(x)x = C\left(\frac{e^{-G|x|}}{|x|^Y} 1_{x<0} + \frac{e^{-Mx}}{x^Y} 1_{x>0}\right) > 0 \text{ for all } x \in \mathbb{R}$$

and

$$k'_X(x) = C\left[\frac{e^{-G|x|}}{|x|^Y}\left(G + \frac{Y}{|x|}\right)1_{x<0} - \frac{e^{-Mx}}{x^Y}\left(M + \frac{Y}{x}\right)1_{x>0}\right]$$

implying that $k(x)$ is increasing on $(-\infty, 0)$ and decreasing on $(0, \infty)$ when $Y > 0$, hence satisfies sufficient selfdecomposability conditions.

For the case of the CGMY subordinator, we have from (21) that the Lévy density can be rewritten in terms of the confluent hypergeometric function of the second kind, $U(a, b, c)$, (see Gradshteyn and Ryzhik, 2007, p. 1023 and 1028) as

$$s(z) = \frac{\Gamma(Y)}{\Gamma(Y/2)\,2^{Y-1}} e^{\frac{z}{2}(\theta^2 - \tilde{\theta}^2)} U\left(Y/2, 1/2, z\tilde{\theta}^2/2\right).$$

It follows that

$$k_Z(z) = \nu_Z(z)z = s(z)\nu_0(z)z > 0$$

and

$$\begin{aligned} k'_Z(z) &= -\frac{1}{4}\left[\frac{2Y}{z} + 2(\tilde{\theta}^2 - \theta^2) + \frac{\sqrt{2}Y\tilde{\theta}}{\sqrt{z}}\frac{U(Y/2 + 1/2, 1/2, z\tilde{\theta}^2/2)}{U(Y/2, 1/2, z\tilde{\theta}^2/2)}\right] k_Z(z) \qquad \text{(B.1)} \\ &= -\frac{1}{4}\left[\frac{2Y}{z} + 2(\tilde{\theta}^2 - \theta^2) + \frac{2Y\tilde{\theta}}{\sqrt{z}}\frac{h_{-Y-1}(\tilde{\theta}\sqrt{z})}{h_{-Y}(\tilde{\theta}\sqrt{z})}\right] k_Z(z), \qquad \text{(B.2)} \end{aligned}$$

which is negative on $(0, \infty)$ when $Y > 0$ since $\tilde{\theta} > \theta, \tilde{\theta} > 0$ (for equalities B.1–B.2, see Abramowitz and Stegun, 1968, p. 505 and 507).

References

Abramowitz, M., & Stegun, I.A. (1968). Handbook of Mathematical Functions with Formulas, Graphs and Mathematical Tables. New York: Dover.

Asmussen, S., & Rosiński, J. (2001). Approximation of small jumps of Lévy processes with a view towards simulation. Journal of Applied Probability, 38, 482–493.

Baeumer, B., & Meerschaert, M.M. (2010). Tempered stable Lévy motion and transient super-diffusion. Journal of Computational and Applied Mathematics, 233, 2438–2448.

Ballotta, L., & Bonfiglioli, E. (2013). Multivariate asset models using Lévy processes and applications (working paper). Cass Business School, City University London.

Borovkova, S., & Permana, F.J. (2010). Asian basket options and implied correlations in energy markets (working paper). Vrije Universiteit Amsterdam.

Broadie, M., & Kaya, O. (2006). Exact simulation of stochastic volatility and other affine jump diffusion processes. Operations Research, 54, 217–231.

Cai, N., Kou, S.G., & Liu, Z. (2013). A two-sided Laplace inversion algorithm with computable error bounds and its applications in financial engineering. Advances in Applied Probability (forthcoming).

Carr, P., Geman, H., Madan, D.B., & Yor, M. (2002). The fine structure of asset returns: An empirical investigation. Journal of Business, 75, 305–332.

Carr, P., Geman, H., Madan, D.B., & Yor, M. (2003). Stochastic volatility for Lévy processes. Mathematical Finance, 13, 345–382.

Černý, A., & Kyriakou, I. (2011). An improved convolution algorithm for discretely sampled Asian options. Quantitative Finance, 11, 381–389.

Chen, Z., Feng, L., & Lion, X. (2012). Simulating Lévy processes from their characteristic functions and financial applications. ACM Transactions on Modeling and Computer Simulation, 22, 14:1–14:26.

Chung, S.-L., Ko, K., Shackleton, M.B., & Yeh, C.-Y. (2010). Efficient quadrature and node positioning for exotic option valuation. Journal of Futures Markets, 30, 1026–1057.

Cont, R., & Tankov, P. (2004). Financial Modelling with Jump Processes. Boca Raton: Chapman & Hall/CRC Press.

Devroye, L. (1981). On the computer generation of random variables with a given characteristic function. Computers and Mathematics with Applications, 7, 547–552.

Fang, F., & Oosterlee, C.W. (2008). A novel pricing method for European options based on Fourier-Cosine series expansions. SIAM Journal on Scientific Computing, 31, 826–848.

Feng, L., & Linetsky, V. (2008). Pricing discretely monitored barrier options and defaultable bonds in Lévy process models: a fast Hilbert transform approach. Mathematical Finance, 18, 337–384.

Glasserman, P., & Kim, K. (2009). Gamma expansion of the Heston stochastic volatility model. Finance and Stochastics, 15, 267–296.

Glasserman, P., & Liu, Z. (2010). Sensitivity estimates from characteristic functions. Operations Research, 58, 1611–1623.

Goldberg, R. (1961). Fourier Transforms. Cambridge Tracts in Mathematics and Mathematical Physics, No. 52. Cambridge: Cambridge University Press.

Gradshteyn, I.S., & Ryzhik, I.M. (2007). Table of Integrals, Series, and Products. New York: Academic Press.

Hughett, P. (1998). Error bounds for numerical inversion of a probability characteristic function. SIAM Journal on Numerical Analysis, 35, 1368–1392.

Kawai, R., & Masuda, H. (2011). On simulation of tempered stable random variates. Journal of Computational and Applied Mathematics, 235, 2873–2887.

Lord, R., Fang, F., Bervoets, F., & Oosterlee, C.W. (2008). A fast and accurate FFT-based method for pricing early-exercise options under Lévy processes. SIAM Journal on Scientific Computing, 30, 1678–1705.

Luciano, E., & Semeraro, P. (2010). Multivariate time changes for Lévy asset models: Characterization and calibration. Journal of Computational and Applied Mathematics, 233, 1937–1953.

Madan, D.B., & Yor, M. (2008). Representing the CGMY and Meixner Lévy processes as time changed Brownian motions. Journal of Computational Finance, 12, 27–47.

Poirot, J., & Tankov, P. (2006). Monte Carlo option pricing for tempered stable (CGMY) processes. Asia-Pacific Financial Markets, 13, 327–344.

Rosiński, J. (2007). Tempering stable processes. Stochastic Processes and their Applications, 117, 677–707.

Sato, K. (1999). Lévy Processes and Infinitely Divisible Distributions. Cambridge: Cambridge University Press.

Wang, X., & Sloan, I.H. (2011). Quasi-Monte Carlo methods in financial engineering: an equivalence principle and dimension reduction. Operations Research, 59, 80–95.

Table I

Grid parameters for CDF Fourier inversion formula.

set	ϵ	CGMY									CGMY subordinator		
		$t=1$			$t=1/12$			$t=1/52$			$t=1$		
		D	L	$\log_2 N$	D	L	$\log_2 N$	D	L	$\log_2 N$	D	L	$\log_2 N$
	10^{-3}	7.0	85	8	7.1	1.2×10^4	15	7.1	3.0×10^5	20	58	1.1×10^4	18
	10^{-4}	9.3	116	9	9.4	1.6×10^4	16	9.4	3.9×10^5	21	74	1.7×10^4	19
	10^{-5}	11.6	151	10	11.7	2.1×10^4	17	11.8	5.0×10^5	21	91	2.6×10^4	20
	10^{-6}	13.9	189	10	14.1	2.6×10^4	17	14.1	6.1×10^5	22	107	3.7×10^4	21
I	10^{-7}	16.2	230	11	16.4	3.2×10^4	18	16.4	7.3×10^5	22	123	5.1×10^4	21
	10^{-8}	18.5	275	11	18.7	3.9×10^4	18	18.8	8.6×10^5	23	139	6.8×10^4	22
	10^{-9}	20.9	324	12	21.1	4.6×10^4	19	21.1	1.0×10^6	23	159	8.9×10^4	23
	10^{-10}	23.2	376	12	23.4	5.3×10^4	19	23.5	1.1×10^6	23	174	1.2×10^5	23
	10^{-13}	30.1	555	13	30.2	7.8×10^4	20	30.6	1.6×10^6	24	222	2.2×10^5	24
	10^{-3}	11.6	20	8	11.6	107	9	11.6	298	10	58	707	14
	10^{-4}	13.9	24	8	13.9	123	9	13.9	339	11	74	841	15
	10^{-5}	16.2	27	8	16.2	138	10	16.2	377	11	91	1010	15
	10^{-6}	18.5	31	8	18.5	152	10	18.5	411	12	107	1158	16
II	10^{-7}	20.8	34	8	20.8	165	11	20.8	444	12	123	1332	16
	10^{-8}	23.1	37	9	23.1	176	11	23.1	477	12	140	1490	17
	10^{-9}	25.4	40	9	25.4	188	11	25.4	508	12	159	1662	17
	10^{-10}	27.7	43	9	27.7	200	11	27.7	539	13	174	1828	17
	10^{-13}	34.6	52	10	34.6	234	12	34.6	624	13	222	2370	18

Grid parameters computed given tolerance level ϵ of total error (regularization, truncation of state and Fourier domains, discretization) in numerical Fourier inversion (see Sections 4.2.1–4.2.4). Process parameters (see Eqs. 19, 20): sets I & II, $t = 1, 1/12, 1/52$. $[-D/2, D/2]$: truncated domain of CDF; $[-L/2, L/2]$: truncated domain of Fourier transform (6); N: number of grid points.

Table II

MC-FT price estimates of European vanilla put, Asian call and UOC barrier options.

set	K	Vanilla put option					Asian call option			UOC barrier option		
		ref. price	MC-FT1 price	std error	MC-FT2 price	std error	ref. price	MC-FT1 price	std error	ref. price	MC-FT1 price	std error
	80	6.3037	6.2757	0.0130	6.3101	0.0130	23.0533	23.0344	0.0234	8.8650	8.8804	0.0132
I	90	9.6597	9.6710	0.0164	9.6677	0.0164	15.5249	15.5049	0.0220	5.2601	5.2579	0.0095
	100	14.0691	14.0516	0.0197	14.0604	0.0197	9.6434	9.6490	0.0197	2.6325	2.6389	0.0062
	110	19.5655	19.5340	0.0229	19.5793	0.0230	5.8405	5.8105	0.0176	0.9894	0.9902	0.0032
	120	26.0513	26.0483	0.0258	26.0527	0.0258	3.6888	3.6987	0.0164	0.1959	0.1975	0.0011
	80	7.0254	7.0401	0.0125	7.0226	0.0124	23.1589	23.1803	0.0244	4.9206	4.9157	0.0104
II	90	10.9517	10.9548	0.0160	10.9355	0.0160	16.2348	16.2145	0.0221	2.7331	2.7361	0.0072
	100	15.8165	15.8150	0.0195	15.8212	0.0195	10.9197	10.9561	0.0195	1.2983	1.3031	0.0045
	110	21.5315	21.5440	0.0229	21.4762	0.0229	7.1342	7.1385	0.0166	0.4734	0.4723	0.0023
	120	27.9847	28.0039	0.0261	27.9752	0.0261	4.5866	4.5824	0.0138	0.0944	0.0953	0.0007

MC-FT prices and standard errors computed using 10^6 simulation trials. Reference prices for the plain vanilla put, Asian call, UOC barrier options obtained respectively using the methods of Fang and Oosterlee (2008), Černý and Kyriakou (2011) and Lord et al. (2008). CGMY parameters: sets I & II. CDF error tolerance: $\epsilon = 10^{-10}$. Other parameters: $S(0) = 100$, $B = 130$, $r = 0.04$, $q = 0.0$, $T = 1$, $n = 12$.

Table III

3-dimensional CGMY process: parameters set.

				125-day correlation		
	asset	$S(0)$	q	F	ABT	BAX
(a) Valuation date: 30.09.2008	F	5.20	0.0%	100%		
	ABT	57.58	2.8%	25%	100%	
	BAX	65.67	1.5%	30%	64%	100%
(b) Margin process		C_j		3.1852	0.5263	0.6017
		G_j		5.7670	8.9598	11.0817
		M_j		12.1599	24.9805	29.8549
		Y		0.8999	0.8999	0.8999
		Calibration RMSE		1.12×10^{-1}	4.15×10^{-1}	4.32×10^{-1}
(c) Idiosyncratic process		C_{Lj}		2.7679	0.2422	0.2880
		G_{Lj}		5.7670	8.9598	11.0817
		M_{Lj}		12.1599	24.9805	29.8549
		Y		0.8999	0.8999	0.8999
		a_j		1.0239	0.6681	0.7457
(d) Systematic process		C_L			0.4085	
		G_L			5.9053	
		M_L			16.4643	
		Y			0.8999	
(e) Cumulant error		c_1		8.52×10^{-2}	2.87×10^{-4}	1.51×10^{-2}
		c_2		6.73×10^{-3}	4.82×10^{-4}	1.23×10^{-2}
		c_3		1.02×10^{-3}	7.60×10^{-5}	1.92×10^{-3}
		c_4		2.30×10^{-4}	3.12×10^{-5}	7.59×10^{-4}
(f) Calibration error				3.71×10^{-3}	-7.73×10^{-3}	-2.30×10^{-1}
(g) Correlation fit error		F		-		
		ABT		6.87×10^{-3}	-	
		BAX		0	1.09×10^{-9}	-

Panel (a). Market data for the three assets considered. Correlation matrix estimated using historical prices of the three assets over a 125-day time window up to (and including) the valuation date. Source: Bloomberg. Panels (b)–(d). Parameters of the CGMY margin processes $X_j(t)$, $j = 1, 2, 3$, and corresponding idiosyncratic and systematic components $L_j(t)$, $j = 1, 2, 3$, and $L_4(t)$. Fit of the multivariate CGMY process tested in panels (e)–(g). Panel (e). Cumulant error expressed as (absolute) difference between the indicated cumulants of the process $X_j(t)$ and the corresponding cumulants of the linear combination $L_j(t) + a_j L_4(t)$ for $j = 1, 2, 3$. Panel (f). Calibration error expressed as difference between the RMSEs generated by calibration to vanilla option market prices of the margins (reported in panel b) and the linear combinations $L_j(t) + a_j L_4(t)$, $j = 1, 2, 3$. Panel (g). Correlation fit error expressed as difference between model and historical correlations. Model correlations computed using (48).

Table IV

Multivariate option contracts: spread option and Asian basket option.

		Crude Monte Carlo		Monte Carlo with antithetic variates		
	K	MC-FT1 price	std error	MC-FT1 price	std error	ref. price
Spread option	20	31.4648	0.0093	31.4682	0.0026	31.4700
	30	21.9351	0.0091	21.9389	0.0027	21.9408
	40	13.1633	0.0082	13.1664	0.0036	13.1686
	50	6.4404	0.0064	6.4400	0.0045	6.4431
Asian basket option	20	22.3345	0.0037	22.3410	0.0010	
	30	12.6770	0.0037	12.6832	0.0010	
	40	3.8684	0.0029	3.8737	0.0015	
	50	0.2773	0.0008	0.2785	0.0008	

Prices and standard errors obtained for 2×10^6 simulation trials using crude MC-FT1, and 10^6 simulation trials using MC-FT1 with antithetic variates. CPU times (in seconds): spread option: 2.75 (crude MC-FT1), 2.53 (MC-FT1 with antithetic variates); Asian basket option: 51.31 (crude MC-FT1), 44.62 (MC-FT1 with antithetic variates). Reference prices for spread options obtained with the method of Lord et al. (2008). Model parameters: Table III. CDF error tolerance: $\epsilon = 10^{-10}$. Other parameters: $r = 0.0336$ (source: Bloomberg), $T = 1$, $n = 12$, $d = 2$ (spread option), $d = 3$ (Asian basket option).

Figure 1

Speed and accuracy of the MC-FT1 & MC-FT2 methods: European vanilla put option.

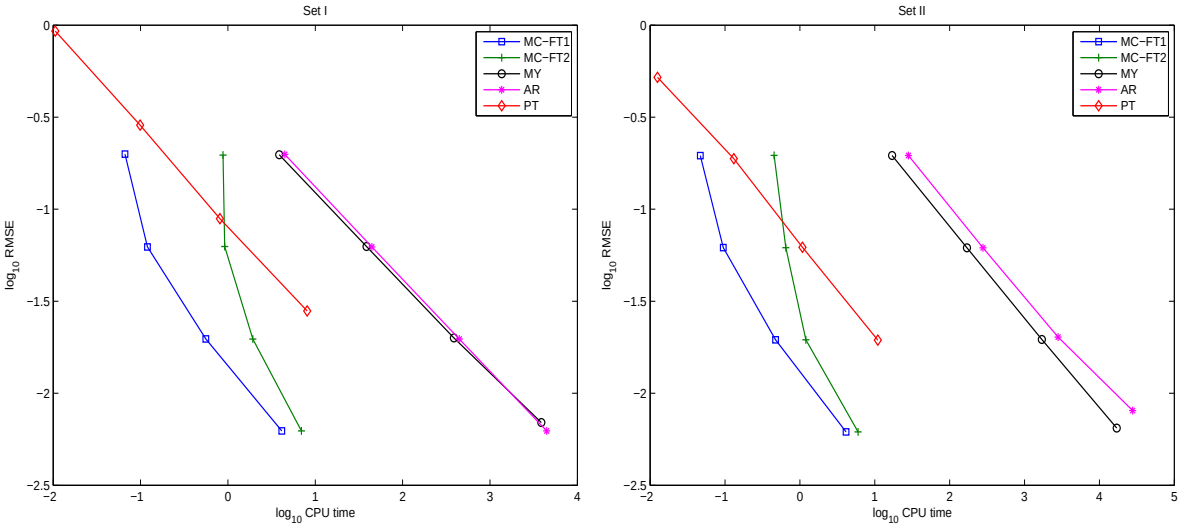

Comparison performed against the PT method Poirot and Tankov (2006), MY method Madan and Yor (2008) and AR method Baeumer and Meerschaert (2010). CGMY parameters: sets I & II. MC-FT CDF error tolerance: $\epsilon = 10^{-10}$. MY parameters: $\varepsilon = 10^{-4}$ (set I) & $\varepsilon = 10^{-5}$ (set II). AR parameter: $\gamma = 2$ (set II). Other parameters: $S(0) = K = 100$, $r = 0.04$, $q = 0.0$, $T = 1$. Simulation trials: $10^4, 10^5, 10^6, 10^7$.

Figure 2

Speed and accuracy of the MC-FT1 method: Asian call option.

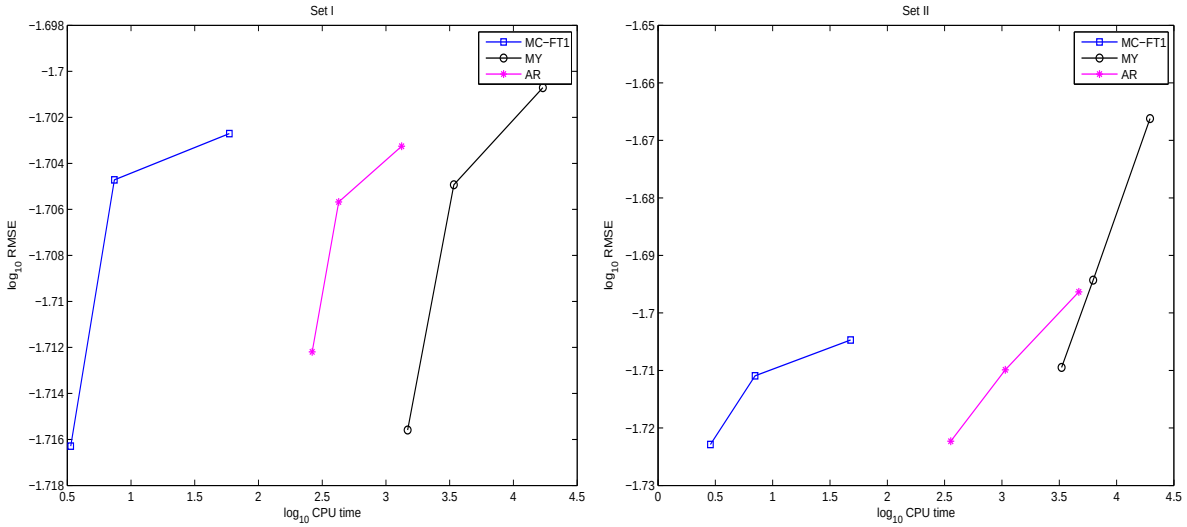

CGMY parameters: sets I & II. MC-FT CDF error tolerance: $\epsilon = 10^{-10}$. MY parameters: $\varepsilon = 10^{-4}$ (set I) & $\varepsilon = 10^{-5}$ (set II). AR parameter: $\gamma = 0.5$ (set II). Other parameters: $S(0) = K = 100$, $r = 0.04$, $q = 0.0$, $T = 1$. Simulation trials: 10^6. Monitoring dates $n = 4, 12, 52$.

Figure 3

Speed and accuracy of the MC-FT1 method: UOC barrier option.

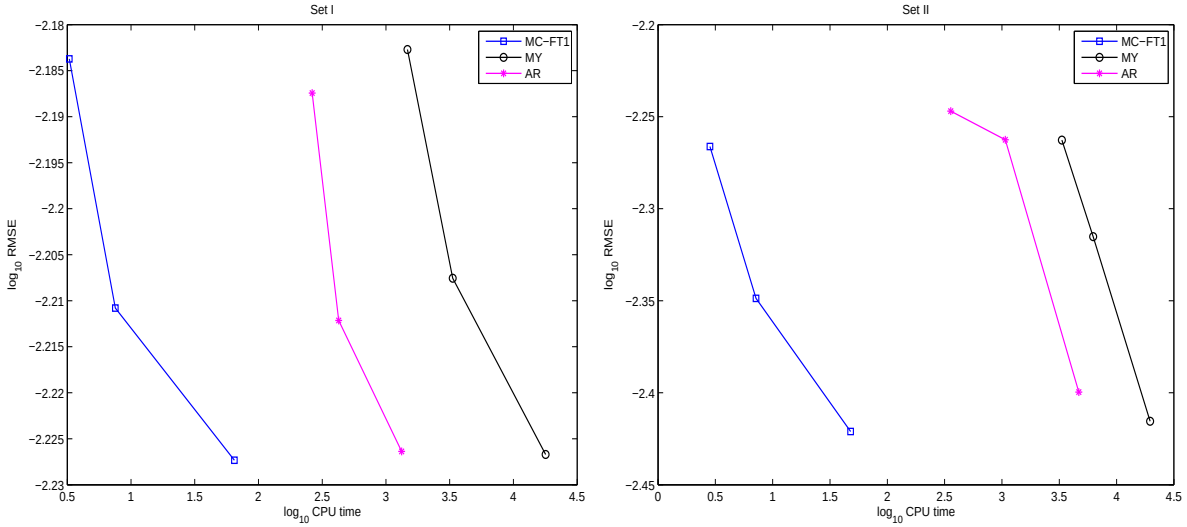

CGMY parameters: sets I & II. MC-FT CDF error tolerance: $\epsilon = 10^{-10}$. MY parameters: $\varepsilon = 10^{-4}$ (set I) & $\varepsilon = 10^{-5}$ (set II). AR parameter: $\gamma = 0.5$ (set II). Other parameters: $S(0) = K = 100$, $B = 130$, $r = 0.04$, $q = 0.0$, $T = 1$. Simulation trials: 10^6. Monitoring dates $n = 4, 12, 52$.